State of Oregon
Department of Geology and Mineral Industries
Vicki S. McConnell, State Geologist

**Open-File Report O-08-12**

# PREHISTORIC CASCADIA TSUNAMI INUNDATION AND RUNUP AT CANNON BEACH, CLATSOP COUNTY, OREGON

By
Robert C. Witter[1]

With contributions by
Curt D. Peterson[2], Kenneth M. Cruikshank[2], Eileen Hemphill-Haley[3], Robert B. Schlichting[4], and Jonathan C. Allan[1]

2008

[1]Oregon Department of Geology and Mineral Industries, Coastal Field Office, 313 SW 2nd St., Suite D, Newport, Oregon 97365
[2]Portland State University, Department of Geology, P. O. Box 751, Portland, Oregon 97207
[3]Department of Geology, Humboldt State University, Arcata, California 95521
[4]Cleveland High School, Portland, Oregon 97202

**NOTICE**

**The results and conclusions of this report are necessarily based on limited geologic and geophysical data. At any given site in any map area, site-specific data could give results that differ from those shown in this report. This report cannot replace site-specific investigations. The hazards of an individual site should be assessed through geotechnical or engineering geology investigation by qualified practitioners.**

**Cover photo:** Oblique aerial photograph of the lower Ecola Creek valley at Cannon Beach, Oregon. (Photo by Alfred A. Aya, Jr., circa 1996).

Oregon Department of Geology and Mineral Industries Open-File Report O-08-12
Published in conformance with ORS 516.030

---

For copies of this publication or other information about Oregon's geology and natural resources, contact:

Nature of the Northwest Information Center
800 NE Oregon Street #5
Portland, Oregon 97232
(503) 872-2750
http://www.naturenw.org

or these DOGAMI field offices:

Baker City Field Office
1510 Campbell St.
Baker City, OR 97814-3442
Telephone (541) 523-3133
Fax (541) 523-5992

Grants Pass Field Office
5375 Monument Drive
Grants Pass, OR 97526
Telephone (541) 476-2496
Fax (541) 474-3158

For additional information:
Administrative Offices
800 NE Oregon St. #28, Ste. 965
Portland, OR 97232
Telephone (971) 673-1555
Fax (971) 673-1562
http://www.oregongeology.com
http://egov.oregon.gov/DOGAMI/

# TABLE OF CONTENTS



# LIST OF FIGURES

## List of Figures, continued.



## LIST OF TABLES

# INTRODUCTION

Many communities located in exposed, low-elevation areas along the Oregon coast face the risk of tsunami inundation. The hazard comes from two principal sources: distant tsunamis that cross the Pacific Ocean produced by earthquakes far from Oregon, and local tsunamis spawned by earthquakes on the Cascadia subduction zone. Local Cascadia tsunamis pose the greatest hazard to people living along the Oregon coast. The Cascadia subduction zone includes the region of deformation that accommodates the convergence between tectonic plates beneath the Pacific Ocean and the North American continent. Within this zone of deformation, the principal source of infrequent, but very large (magnitude 9) earthquakes is a 1,000-km-long thrust fault that extends from Cape Mendocino, California, to Vancouver Island, British Columbia, and projects to the seafloor at the base of the continental slope (Figure 1). Seafloor uplift caused by the most recent Cascadia earthquake in 1700 produced a tsunami that damaged villages in Japan (Satake and others, 1996) and provides the foundation for native American legends (Ludwin and others, 2005). Geologic evidence of drowned wetlands and widespread sand sheets interlayered with sediments beneath estuaries and coastal lakes above the Cascadia subduction zone warn of repeated magnitude 9 earthquakes that triggered at least 13 tsunamis over the last 4,600 years (Atwater and Hemphill-Haley, 1997; Clague and others, 2000; Witter and others, 2003; Kelsey and others, 2005). A longer record of 20 undersea landslides triggered by Cascadia earthquakes spans the last 10,000 years and implies that tsunamis that accompany these events occur on average every 500 years (Goldfinger and others, 2003).

As of the date of this report, published tsunami inundation maps that predict the severity of ocean flooding cover less than one third of Oregon's coastal communities that reside in the path of potentially devastating Cascadia tsunamis. In addition, new earthquake source models (Tsunami Pilot Study Working Group, 2006) developed since the 2004 Indian Ocean tsunami question the veracity of existing tsunami hazard maps (e.g., Priest and others, 1997a, 1997b, 2002, 2003; Walsh and others, 2000) and suggest that present estimates may significantly underestimate potential runup elevations and inland inundation (Figure 2). Extensive sand sheets documented at numerous sites in Oregon, including the lower Ecola Creek valley at Cannon Beach, provide tangible evidence of the impact and extent of prehistoric tsunamis that have invaded the coast, but such crucial information has largely been ignored by efforts to simulate tsunamis numerically. These deficiencies in current assessments of tsunami hazards highlight a critical need for a new approach that uses geologic evidence of prehistoric tsunami inundation to evaluate the validity of earthquake source models and computer simulations that predict tsunami inundation hazard.

This report summarizes the results of the geologic component of a comprehensive tsunami hazard assessment for Cannon Beach, Oregon (Zhang and others, 2007; Priest and others, 2008). The purpose of the geologic investigation is to map the landward extent of sand deposits left by Cascadia tsunamis that inundated the lower Ecola Creek valley over the last 2,000 years. Fossil diatom assemblages and sand mineralogy, among a variety of criteria, provide data that distinguish sand layers deposited by tsunamis from deposits that record river flooding. Sand deposits left by ancient tsunamis are used to constrain model-based estimates of tsunami inundation by providing empirical evidence of the runup elevations and extents of inundation reached by prehistoric Cascadia tsunamis. A related study investigated possible flow paths and minimum runup elevations of prehistoric tsunamis at Cannon Beach (Peterson and others, 2008).

## History and setting of the lower Ecola Creek valley

The Ecola Creek watershed covers 5,700 ha; the entire area lies within 10 km of the Pacific Ocean (Parker and others, 2001). Forests cover about 95 percent of the watershed, and most of these lands are managed by commercial timber companies. Historically, the Ecola Creek estuary was much more extensive than today and consisted of a system of tidal channels and wetlands that covered most of the low-lying areas west of Highway 101 in downtown Cannon Beach. In 1806 the creek was named *E-Co-La*, or Whale Creek, by Captain William Clark while seeking to trade with Salish-speaking people for whale oil and blubber (O'Donnell, 1996). Permanent urban development beginning in 1890 has gradually encroached on the estuary and reduced

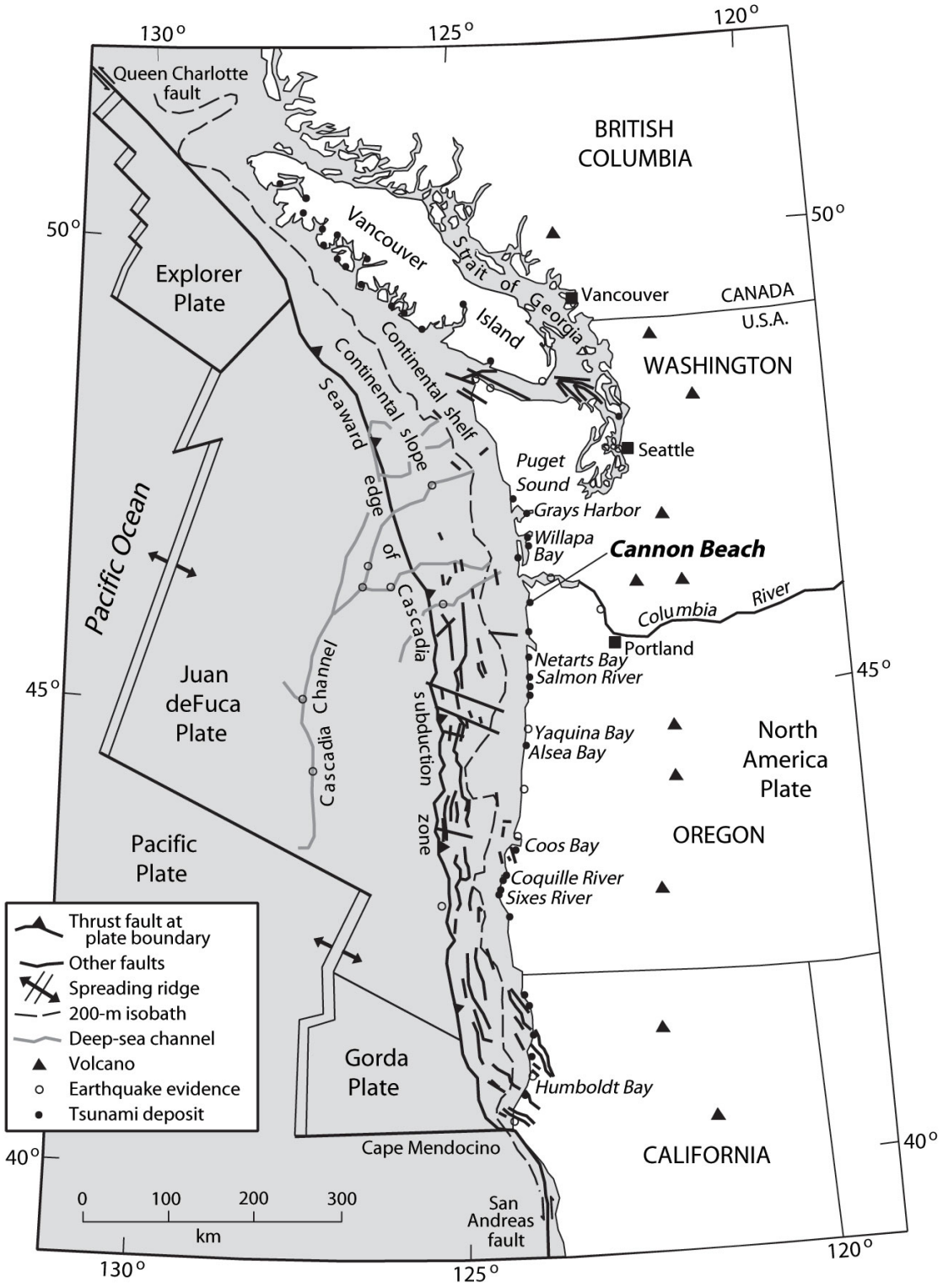


**Figure 1.** Tectonic setting of the Pacific Northwest region of the United States showing the Cascadia subduction zone and other plate boundaries, Quaternary faults in the North American plate, and the location of the study site at Cannon Beach in northwestern Oregon (modified from Nelson and others, 2004). The deformation front (barbed line) is defined by bathymetry where the abyssal plain meets the continental slope and is inferred to represent the surface projection of the Cascadia thrust fault. Open and closed circles represent sites with evidence for prehistoric Cascadia earthquakes and tsunamis. Closed circles mark sites with deposits interpreted to record tsunami inundation caused by a magnitude 9 Cascadia earthquake on January 26, 1700 (Satake and others, 1996).

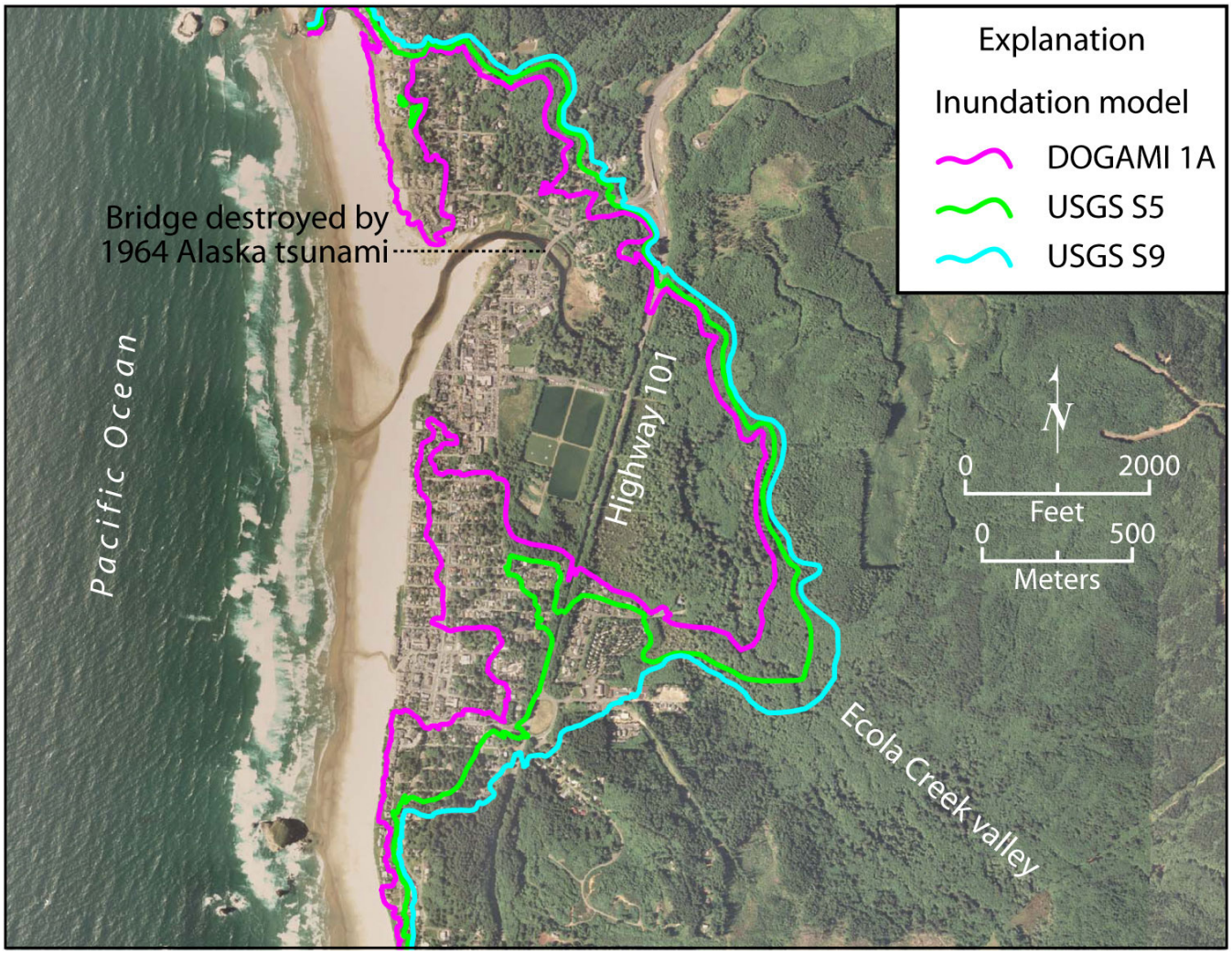


**Figure 2.** Comparison of existing numerical tsunami inundation models at Cannon Beach, Oregon. Each model used a numerical grid based on 10-m topographic data. Model 1A was developed by DOGAMI (Priest and others, 1997a) to create tsunami hazard maps for several areas along the Oregon coast. Higher runup and more extensive inundation is predicted by simulations that use source models developed for the Seaside, Oregon, Tsunami Pilot Study (Tsunami Pilot Study Working Group, 2006; U.S. Geological Survey models S5 and S9 are from Eric Geist, personal communication, 2006).

the size of the adjacent wetlands (Parker and others, 2001).

Seasonal high flows, extreme ocean levels, and storms commonly caused flooding in the business district of Cannon Beach, particularly during severe storms in 1939 and 1967. Strong westerly winds produced by the storm in 1967 combined with a very high tide flooded the business district of Cannon Beach to a depth of 2.5 ft (0.8 m) (O'Donnell, 1996). A tsunami generated by an earthquake in Alaska, described in detail below, caused extensive flooding and damage in 1964. Levees, dikes, and riprap constructed for flood control purposes and the construction of U.S. Highway 101 in 1950 have permanently altered the hydrology of the estuary. Construction of two wastewater treatment lagoons, several culverts, and a tide gate along the 2nd Street levee in 1958 disconnected wetlands south of 2nd Street from periodic tidal inundation and high stream flows (Parker and others, 2001). The final levee segment constructed in 1970 between the Ecola Creek bridge and 2nd Street prevented subsequent flooding compounded by high tides and elevated stream flow in downtown Cannon Beach. Despite the extensive urbanization at the mouth of Ecola Creek, some fresh-

water wetlands remain, chiefly east of U.S. Highway 101 and within a small marsh, Pompey Marsh, located between the wastewater ponds and the downtown area. Plants typical of the existing freshwater wetlands along Ecola Creek include Sitka spruce (*Picea sitchensis*), red alder (*Alnus rubra*), willow (*Salix spp.),* slough sedge (*Carex obnupta*), cattail (*Typha spp.*), soft rush (*Juncus effusus*), reed canarygrass (*Phalaris arundinacea*), and skunk cabbage (*Lysichiton americanum*).

The geology in the Ecola Creek watershed consists of Tertiary marine mudstone invaded by volcanic flows chemically identical to the Grande Ronde basalt of the Columbia plateau (Niem and Niem, 1985). Sedimentary rocks include well-bedded micaceous mudstone and thin beds of feldspathic sandstone that comprise the Cannon Beach member of the middle to lower Miocene Astoria Formation. Rocks of the middle Miocene Grande Ronde basalt invaded the mudstone to form sills and dikes. In higher elevations of the watershed, ancient lava deltas are composed of submarine pillows and basalt breccias. On steeper valley walls landslides are common; in the lowlands of the lower valley surficial deposits include alluvial and marsh sediments and beach and dune sand (Figure 5).

## Impact of the 1964 Alaska tsunami at Cannon Beach, Oregon

The impact of the 1964 Alaska tsunami at Cannon Beach may portend the consequences of a potentially much larger Cascadia tsunami that could result in more disastrous losses. Approximately four hours after its generation by the magnitude ($M_w$) 9.2 Prince William Sound earthquake, a distant tsunami inundated Cannon Beach on Friday, March 27, 1964, shortly after 11:34 PM local time (Lander and others, 1993) during a rising tide (*The Sunday Oregonian,* March 29, 1964, p. 40). Reports of the impacts of the tsunami at Seaside, 13 km to the north, indicate that the first surge was preceded by a troughlike depression that caused the ocean to withdraw to an elevation of less than −2 ft (−0.6 m) below mean lower low water (MLLW) as inferred from eyewitness observations (Horning, 2006). Horning (2006) reported runup elevations that ranged from 22 to 26 ft (6.7 to 7.9 m) (MLLW) for the first surge along the ocean front at Seaside. From eyewitness reports, slightly lower runup elevations were reached by the initial waves at Cannon Beach. Wave runup at the ocean front did not exceed 20 ft (6.1 m) (MLLW) because there are no reports or other evidence to suggest the tsunami overtopped the barrier spit that fronts the beach and rises to elevations of 20 to 23 ft (6.1 to 7.0 m) (MLLW). Newspaper reports of water depths at two sites (Table 1) suggest minimum water elevations in Cannon Beach

**Table 1.** Eyewitness water depth observations and minimum water level elevations during the 1964 Alaska tsunami at Cannon Beach, Oregon.

| Site | Water Depth (ft) [m]* | Information Source | Elevation of Site: NGVD 29 (ft) [m]# | Elevation of Site: NAVD 88 (ft) [m]† | Water Level, MLLW (ft) [m]§ |
|---|---|---|---|---|---|
| Bell Harbor Motel | 5 [1.5] | *The Sunday Oregonian,* March 29, 1964, p. 40 | 12 [3.6] | 15.5 [4.7] | 20 [6.1] |
| Steidel house | 2.5 [0.8] | *Seaside Signal*, April 2, 1964, p. 1 | 13 [4.0] | 16.5 [5.0] | 19 [5.8] |
| Downtown Cannon Beach | 1 [0.3] | *Seaside Signal*, April 2, 1964, p. 1 | 9 [2.7] | 12.5 [3.8] | 13 [4.0] |

* Water depth estimates based on eyewitness observations noting water damage and water marks on buildings and depth of flooding along the main street in downtown Cannon Beach.

\# Site elevations (accurate to ±1 ft [0.3 m]) determined from 2-ft-contour map referenced to the National Geodetic Vertical Datum of 1929 (NGVD 29) vertical datum provided by the City of Cannon Beach.

† Elevations corrected to the North American Vertical Datum of 1988 (NAVD 88) by the addition of 3.5 ft (1.1 m) to the NGVD 29 elevation.

§ Minimum water level elevation estimate relative to the mean lower low water (MLLW) tidal datum is equal to the sum of the observed water depth and the NAVD 88 elevation of the site minus 0.2 ft (<0.1 m), the difference between MLLW and NAVD 88 datums at the Astoria tidal benchmark (Station 9439040). All values rounded to the nearest foot.

reached 19 to 20 ft (5.8 to 6.1 m) (MLLW). A second surge reached lower elevations at Cannon Beach at around 3:30 AM but caused little or no damage (*The Sunday Oregonian,* March 29, 1964, p. 40).

At Cannon Beach the 1964 tsunami damaged city infrastructure at a cost of $50,000 and caused $180,000 (over $0.35 million and $1.27 million in 2008 dollars, respectively) in losses to private property based on estimates from the Oregon State Civil Defense Agency in April 1964 (Spaeth and Berkman, 1967). Photographs exemplify the tsunami's impact (Figure 3). The most dramatic impact involved the complete destruction of the city's primary bridge across Elk Creek, now named Ecola Creek, that was captured in a photograph and newspaper headline published in the *Hillsboro Argus* on March 30, 1964 (Figure 3a). The photograph clearly shows the remains of the 200-ft- (~60-m-) long bridge deck dismembered by the tsunami into two sections and deposited approximately 900 ft (275 m) upstream in a low-lying meadow on the northeast bank of the

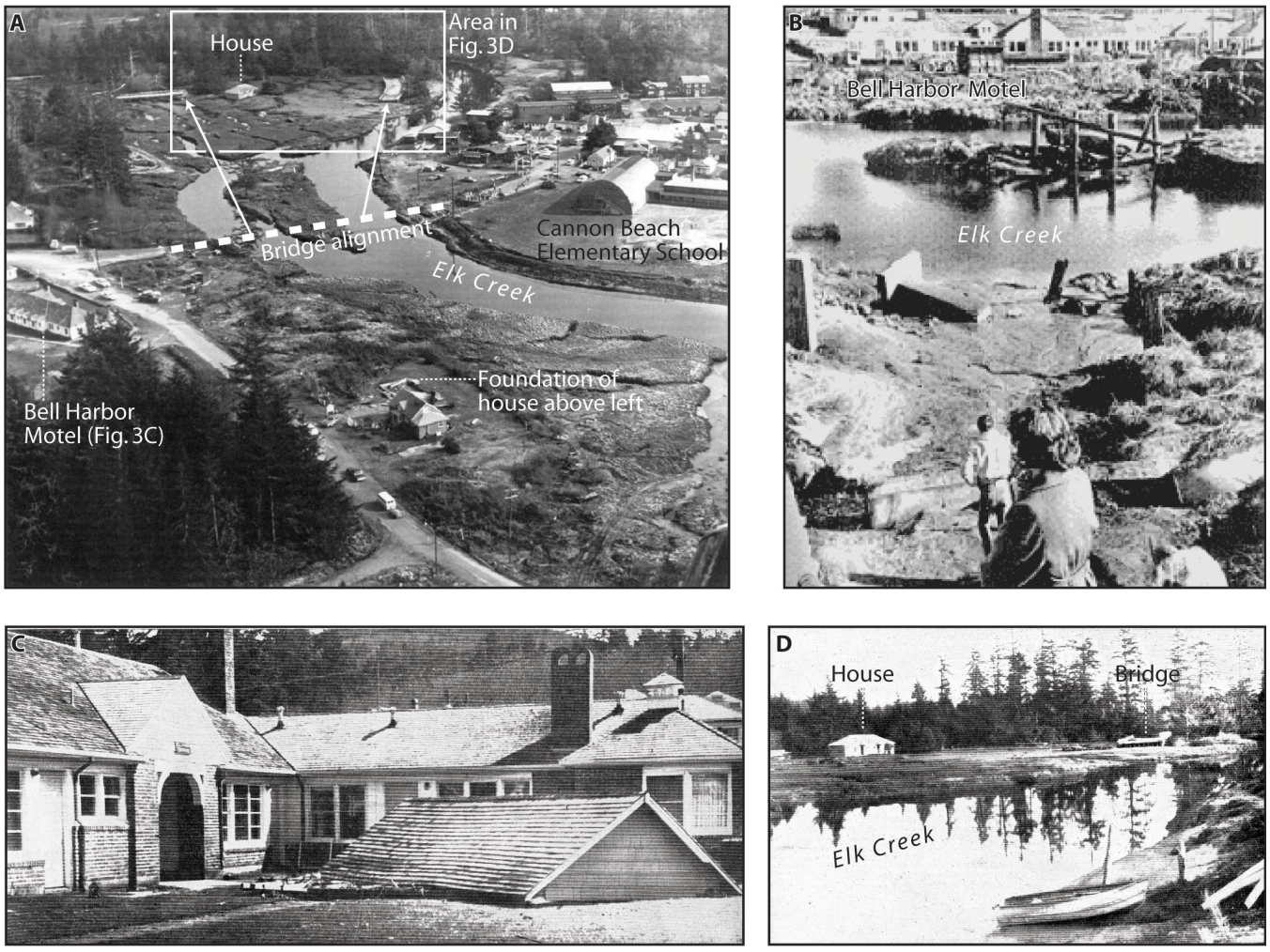


**Figure 3.** Photographs showing the impact of the March 27, 1964, Alaska tsunami (courtesy of the Cannon Beach Historical Society).
(A) Oblique aerial photograph of the lower Elk Creek valley (now Ecola Creek) that flows through downtown Cannon Beach. Decking from the old Elk Creek bridge was torn from its abutments and transported 300 m upstream. A foundation in the lower part of the photo marks the original position of a house that was carried 400 m upstream and deposited between the bridge sections.
(B) View to the northwest across Elk Creek showing bridge pilings and piers, all that remained after the tsunami destroyed the Elk Creek bridge in 1964. Bell Harbor Motel can be seen in the distance across the creek.
(C) Bell Harbor Motel suffered considerable damage from flooding during the tsunami, including broken windows, water damage, and destruction caused by drift logs. The roof of a another building was left in the front yard of the motel after being carried several hundred yards by waves.
(D) View to the southeast looking across Elk Creek at the bridge remains and house transported hundreds of meters inland by the tsunami.

creek. Further impacts of the wave included extensive damage to the Bell Harbor Motel caused by a 16-ft- (4.9-m-) long drift log borne by strong currents (*Seaside Signal*, April 2, 1964, p. 1) as well as interior water damage and the costs of removing debris (Figures 3b and 3c). The force of the wave also ripped one unit of the Buoys and Gulls Motel off its foundation, transporting the structure approximately 1,500 ft (460 m) inland (*Seaside Signal*, April 2, 1964, p. 7) to rest between the two bridge sections (Figure 3d).

Scant reports provide few constraints on the range of flow depths of the 1964 tsunami and the extent of its inundation. For example, eyewitnesses contend that water depths reached 5 ft (1.5 m) at the Bell Harbor Motel (*The Sunday Oregonian,* March 29, 1964, p. 40), 2.5 ft (0.8 m) at a house owned by William and Sally Steidel, and as much as 1 ft (0.3 m) of water on the city's main street after the initial wave (*Seaside Signal*, April 2, 1964, p. 1). One particularly descriptive account of the extent of inundation comes from Schlicker and others (1972, p. 106), who reported flooding of two city blocks in downtown Cannon Beach: "Motels along Elk Creek were badly damaged and much of the business district was flooded. The two business blocks from 1st to 3rd Streets and from Hemlock to Spruce Streets were all under water, as was the area eastward to U.S. Highway 101."

The tsunami inundated at least as far inland (east) as the highway embankment as deduced from reports of damage to the U.S. Highway 101 bridge that crosses Ecola Creek (Figure 4) (Spaeth and Berkman, 1967). However, there are no reports that indicate flooding of Highway 101. The absence of deep grooves or other signs of erosion in the marsh along the transport path followed by sections of the old Elk Creek bridge (Figures 3a and 3d) suggests that flow depths in the Ecola Creek channel were sufficiently deep to float the bridge to its final resting place. If flow depths were less than the height of the bridge deck (1.5 to 3 m) at the location where it finally settled, eroded furrows would have scarred the marsh along the transport path as the decking, propelled by the velocity of the wave, plowed up the channel. One eyewitness (Les Wierson, personal communication, 2008) recounted that water flooded the city from the east as waves inundated the creek and surrounding wetlands, but the tsunami left dry parts of the area, including the main water pump station at 2nd and Spruce Streets and the dikes surrounding two waste water lagoons.

## Prehistoric tsunami deposits at Cannon Beach, Oregon

Gallaway and others (1992) first demonstrated that stratigraphic sequences beneath the lower Ecola Creek valley preserve at least two sand sheets of marine origin that extend over 1 km inland, but these authors did not investigate the total inundation extent by tracking the distribution of sand deposits east of Highway 101. Evidence that the sand came from a marine source includes the presence of rounded pyroxene grains and grain-size distributions found in beach sand that differ from sediment in the active channel of Ecola Creek. Gallaway and others (1992) noted an absence of bedform structures, lack of cross stratification, and the widespread extent that distinguished the sand sheets from discontinuous, laminated sand lenses deposited by extreme storm waves that were observed only within tens of meters near the creek mouth. Instead, Gallaway and others argued that the sand sheets were more likely deposited in the waning stage of turbulent suspensions caused by a tsunami because in some cases a layer of detrital organics, which settled more slowly than fast-settling sand, caps the deposit. Similar distinctions were drawn from comparisons between deposits left by the 2004 Indian Ocean tsunami and deposits emplaced by hurricane Katrina (Moore, 2006). Wetland mud overlying the youngest sand sheet suggests a change in the hydrology of the creek. Gallaway and others suggest that the wetland water table rose in response to a sudden rise in sea level caused by tectonic subsidence during the most recent Cascadia earthquake.

Gallaway and others (1992) provide compelling evidence for a tsunami origin for sand sheets at Cannon Beach, but the precise time of the inundations eluded them. An uncalibrated date of 380 ± 60 $^{14}$C yr BP on detrital wood entombed in the youngest sand layer provides a crude maximum age that predates age estimates of the youngest buried peat horizons and overlying sand deposits documented in adjacent estuaries along 175 km of the northern Oregon coast (Darienzo and Peterson, 1995). Elsewhere, high-precision $^{14}$C ages on earthquake-killed trees and conventional ages on tidal-marsh plants at sites in northern Oregon (Nelson and others, 1995) and numerical models of a tsunami that reached Japan (Satake and others, 1996) link the youngest sand sheet to the 1700 tsunami. $^{14}$C dates on bulk peat sampled directly below the second youngest sand layer range from 1060 ± 50 to 1270 ± 60 $^{14}$C yr BP and


**Figure 4.** Color aerial orthophotograph of Cannon Beach in 2005 showing estimated minimum inundation of the 1964 Alaska tsunami (yellow dashed line) derived from eyewitness observations of water depth (Table 1) and 2-ft (0.6-m) contour lines from a digital elevation model provided by the city of Cannon Beach. The inundation line coincides with the 16-ft (4.9-m) contour line (NGVD 29) along the ocean front and north of Ecola Creek near the Steidel house and Bell Harbor Motel. The 10-ft (~3-m) contour line (NGVD 29) was used to approximate inundation in downtown Cannon Beach and east to U.S. Highway 101. East of the highway the inundation line coincides with the 8-ft (2.4-m) contour line (NGVD 29), but there is no information from which to evaluate the extent of inundation in this area.

generally correlate in time with dates on inferred tsunami deposits found at other northern Oregon sites.

Peterson and others (2008) reevaluated the data of Gallaway and others (1992) and initiated further investigations, including ground-penetrating radar surveys, with the objective of estimating minimum runup elevations for prehistoric Cascadia tsunamis that may or may not have overtopped the barrier sand ridge.

## APPROACH AND METHODS

Field investigations mapped the subsurface stratigraphy beneath the lower Ecola Creek valley and, to a limited extent, within an upland swale in the vicinity of the Cannon Beach City Hall (Figure 5). Field teams used 2.5-cm-diameter gouge cores to determine the presence or absence of sand layers interrupting sequences of freshwater peat and mud deposited beneath the floodplain and wetlands of Ecola Creek. Few natural outcrops along the active creek channel were examined because vegetation or cover material obscured most banks and high ground water obviated shallow shovel pits. Vertical elevation profiles along coring transects were measured with an electronic level and tied to temporary benchmarks. The vertical position of each benchmark (NAVD 88) was derived using a Trimble 5700/5800 Real-Time Kinematic Differential Global Positioning System (GPS). The elevations of less accessible sites or sites with standing water were estimated by interpolation or by surveying the elevation of the contiguous water surface. All field observations, including sediment core logs, photographs, and field site coordinates, were assembled by Peterson and others (2008).

A variety of key sedimentary characteristics have been identified to differentiate tsunami deposits from sand layers that record river floods or storm surges (Peters and others, 2003). For instance, the presence of marine or brackish diatoms in the sand layer has been used to rule out a river source for sand (Hemphill-Haley, 1995). Evidence of landward-directed flow, distinctive sand composition and texture, and geochemical indicators have also been used to infer a marine rather than a river source for sand deposits (e.g., Atwater, 1987; Darienzo and Peterson, 1990; Atwater and Hemphill-Haley, 1997; Benson and others, 1997). Distinguishing tsunami deposits from storm-related deposits is more difficult because both reflect a marine source. However, geologic studies of deposits resulting from both processes suggest that tsunamis leave much more extensive (many hectares) deposits than do localized (less than one hectare) overwash fans deposited by storm waves that overtop barrier spits. Sedimentary characteristics also differ. Tsunami deposits may consist of multiple, thick (several inches), normally graded beds of sand deposited out of suspension possibly from successive giant waves, whereas storm deposits may consist of thinner, cross-laminated deposits with bedform structures that reflect entrainment processes (Tuttle and others, 2004; Nelson and Leclair, 2006). Finally, linking a sand layer to evidence of earthquake-related deformation has also been used to build a case for tsunamis as the best explanation for sand deposits (Atwater, 1987). This study uses sand sheet thickness, trends in grain size, fossil diatom analysis, and sand mineralogy to evaluate the likely origin of sand layers deposited in the lower Ecola Creek valley. From these and other observations I consider ten criteria that support a tsunami origin to assess whether a sand layer was deposited by a prehistoric tsunami or some other process:

1. The sand deposit consists of well-sorted, quartz-rich sand and rounded augite grains;
2. Brackish-marine diatoms are present;
3. The deposit thins and/or sand grain size fines in a landward direction;
4. Normally graded beds and/or mud lamina are present;
5. Rip-up clasts are present;
6. The lower contact of the deposit is sharp or shows evidence of erosion;
7. Organic debris is present at the top of deposit;
8. The deposit extends over hundreds of meters;
9. The deposit coincides with a buried soil subsided by an earthquake;
10. The deposit age overlaps with regional evidence for a Cascadia earthquake or tsunami.

Sand mineralogy and grain size analyses used a standard petrographic microscope (250× magnification) to examine samples from the modern beach and active

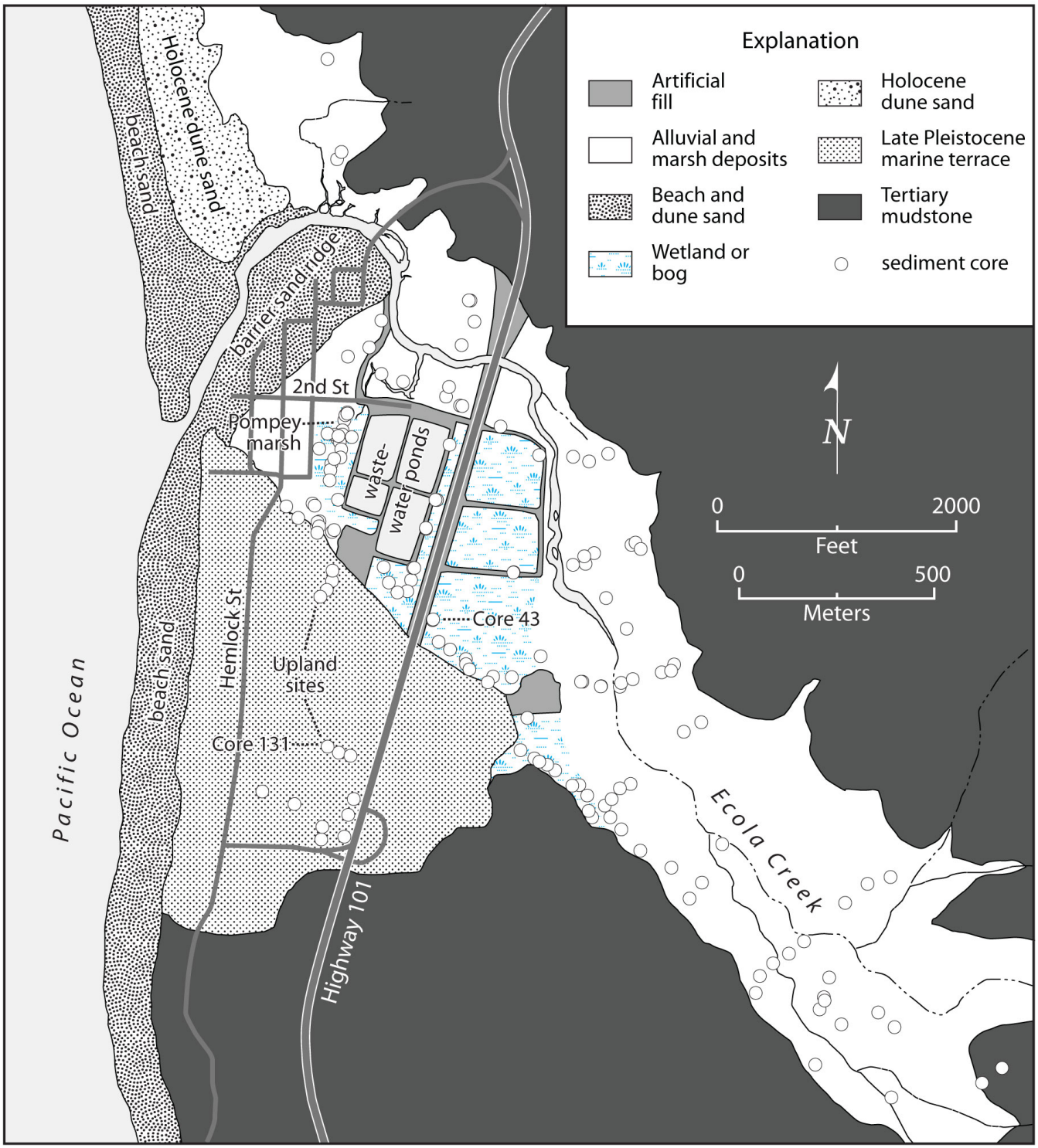


**Figure 5.** Map of the lower Ecola Creek valley and surrounding uplands showing the locations of 160 sediment cores examined for evidence of sand layers deposited by tsunamis or creek floods. Reconnaissance cores at upland sites lacked continuous sand layers. Core 43 was sampled for diatom analyses shown in Figure 18. Quaternary deposits in the valley and along the coast reflect the activity of both fluvial and coastal processes. The uplands surrounding Cannon Beach are chiefly composed of well-bedded mudstone of the middle to lower Miocene Cannon Beach member of the Astoria Formation (Niem and Niem, 1985). Large basaltic dikes and sills that locally invade the mudstone (not shown) have been linked through geochemistry and magnetic polarity to the middle Miocene Grande Ronde Basalt that flowed from the Columbia Plateau (Niem and Niem, 1985).

creek channel as well as samples of four sand layers buried beneath the lower Ecola Creek valley. Floating and decanting removed organics from dried sand samples. The samples were washed through a 4 phi (0.062 mm) wet sieve to separate silt and clay from sand-sized and coarser particles. Mean grain size, standard deviation, and mean normalized standard deviation were determined from measurements of 25 mounted grains on slides prepared from the total sand fraction. Each slide was flipped 90 degrees and reverse counted to check for slide bias. The fine sand-size fraction was separated in Na-polytungstate (2.99 sp g) to isolate augite, a clinopyroxene mineral. Augite is well suited to differentiate littoral (beach) from river sand sources because augite grains in beach sand are rounded, whereas augite grains in river sand are angular (Peterson and Darienzo, 1996). Examination of 100 grains from each heavy-mineral split determined the relative roundness of augite in the sand samples. Some samples contained fewer than 100 augite grains.

Fossil diatoms provide information about the spatial and temporal range of ecological conditions in the lower Ecola Creek valley and the possible sources of sand layers. Our approach uses diatoms to differentiate marine from freshwater deposits by comparing the relative abundances of fresh, brackish, and marine species identified in sand layers to diatom abundances in overlying and underlying peat or mud (Hemphill-Haley, 1996). In particular, elevated abundances of marine taxa in a sand layer, compared to deposits above and below, would be consistent with inundation by ocean waves (e.g., Schlichting and Peterson, 2006). Diatom sample preparation, identification, and counting followed the methods of Hemphill-Haley (1996). For this project, Hemphill-Haley identified and counted 100 valves in each of 12 samples (1 to 2 cc) from a single sediment core located along the southeastern margin of the valley directly west of Highway 101 (Figure 5). She examined samples from four sand layers and from peat and mud above and below each sand deposit. Schlicting focused on identifying and quantifying the number of fossil diatoms present in samples from sand layer 4 at multiple sites (Figure 5). For two sites, he also analyzed samples of mud above and below the sand deposit. Because the samples contained many broken valves and the abundances of intact specimens were generally low (fewer than 36 unbroken valves), Schlichting counted the total number of diatoms from 10 randomly positioned fields of view.

Identifiable plant remains, such as conifer needles, moss, and herbaceous seeds entombed in sand deposits were submitted by DOGAMI to Beta Analytic Inc., Miami, Florida, for radiocarbon dating using the accelerator mass spectrometry (AMS) technique. The plant fossils were removed from samples of sand using a 0 phi (1 mm) wet sieve, cleaned of all sediment and young rootlets, rinsed with tap water, and air dried. Because the sample material is detrital and likely died before being incorporated in the sand deposit, lab-reported conventional radiocarbon ages, calibrated using the computer program Calib Rev 5.0.1 (Stuiver and Reimer, 1993) and the IntCal04 calibration data set of Reimer and others (2004), provide maximum-limiting estimates of the time of sand deposition (Table 3). Metric units of measurement use the International System of Units (SI) except where original maps or other data are in English units (e.g., inches, feet, miles). Where English units are reported, the equivalent metric units are included in parentheses.

## EVIDENCE FOR PREHISTORIC CASCADIA TSUNAMIS

Sediments beneath the floodplain and wetlands of the lower Ecola Creek valley contain four sand sheets interlayered with freshwater peat and mud. Several processes are capable of depositing sand layers in this environment, including high creek flow during floods, ocean storms coincident with high tides and tsunamis, both from distant sources located around the Pacific Ocean, and local Cascadia earthquakes. Cascadia tsunamis best explain three of the most extensive sand sheets with evidence of a beach source transported by marine water. The other sand sheets are best explained by flood-related deposits of Ecola Creek or possibly deposits left by the 1964 Alaska tsunami.

## Stratigraphy and sedimentology of sand layers

The four sand layers correlated in sediment cores across hundreds of meters (Figure 6) are interbedded with mud (clay and silt) and organic deposits (peat and peaty mud) (Figures 7–9). The youngest three sand layers are thickest beneath Pompey Marsh (profile A-A'; Figure 7) and can be tracked for hundreds of meters as they become thinner inland along the southeastern margin of the valley (profile B-B'; Figure 8). All four sand layers were identified in cores west of Ecola Creek but were not present in natural exposures of levee deposits along Ecola Creek (profile C-C'; Figure 9). Only one discontinuous sand deposit (sand layer 4) was identified in floodplain deposits (silt and clay) along the central axis of the valley (profile D-D') and in a cross-valley profile (E-E') located approximately 2.2 km inland from the creek mouth (Figure 8). Photographs of representative sand layers in sediment cores are shown in Figures 10–16. Sand grain size and mineralogy data are presented in Table 2. Characteristics of the sand layers are presented from youngest to oldest in the order they were described in the field.

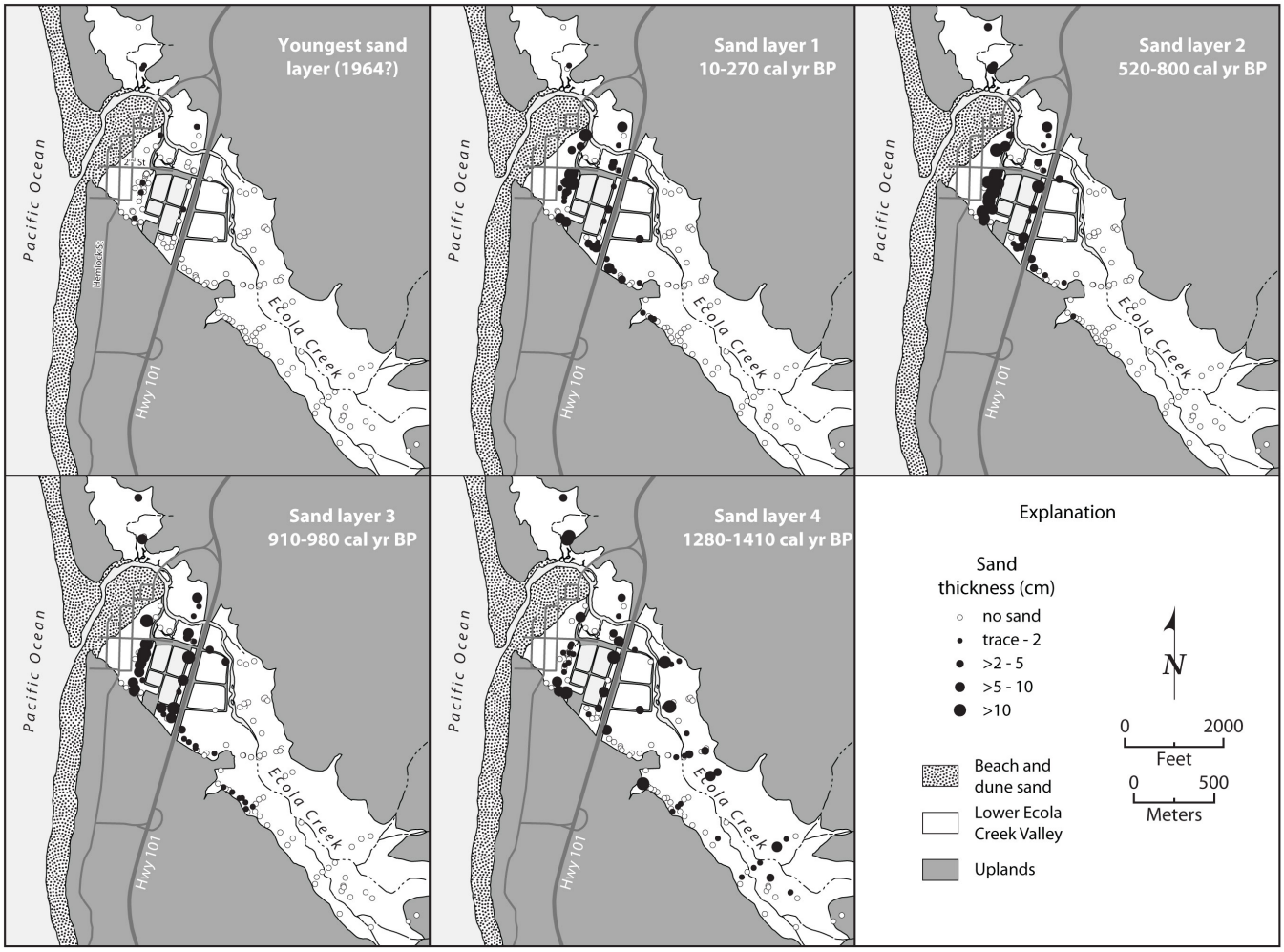


**Figure 6.** Maps of the lower Ecola Creek valley depicting the distribution of five sand deposits correlated among numerous sediment cores (black circles) and shown in stratigraphic profiles (Figures 6–8). Variations in the thickness of each sand layer are indicated by the diameters of black circles. Open circles show cores without a correlative sand layer. Calibrated $^{14}C$ ages are shown for each sand layer (Table 1); the youngest deposit may reflect deposition by the 1964 Alaska tsunami on the basis of historical documents (see discussion in text).

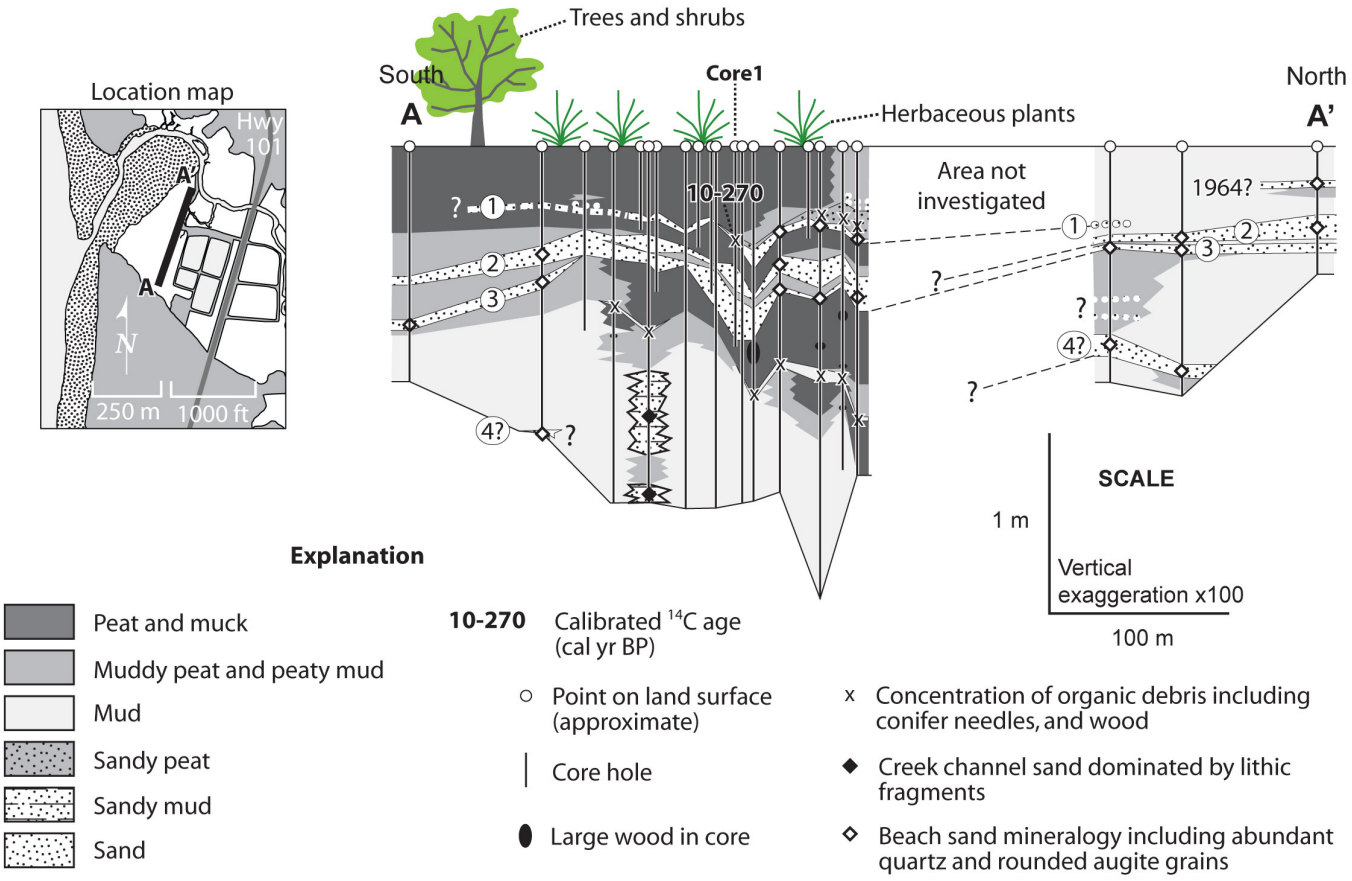


**Figure 7.** Stratigraphic profile A-A' showing five sand layers preserved beneath Pompey Marsh near downtown Cannon Beach.

Sand layer 1 is thickest (> 0.1 m) at Pompey Marsh near the creek mouth (Figures 6 and 7) and thins inland over more than 1.4 km as evident in sediment cores along the southeastern margin of the valley (Figure 8). Distinctive black peat underlies the sand layer across a clear (3 to 10 mm) to sharp (≤ 3 mm) contact aiding in correlation between sites (Figure 10). Field observations note that sand 1 is well sorted and fine grained and consists of abundant quartz grains. In some cores, clasts of peat or inorganic mud mixed in the deposit suggest erosive currents placed the sand. In many cases detrital organic debris was intermixed in the uppermost part of the deposit. Petrological analyses of sand layer 1 (core CANB43B) identify 59 percent of the augite grains as rounded versus 41 percent of the grains as angular. This suggests that the deposit represents a mixture of beach and river sand sources (Table 2).

Less distinct and sometimes thinner, sand layer 2 extends nearly as far inland (1.4 km) as sand 1 (Figures 6 and 7). In many cores a sharp contact separates sand 2 from an underlying thin (<1 in) layer of peat or mud (Figure 11). In other cores the sand 2 deposit could not be distinguished from sand layer 3 because only one deposit was observed over the same stratigraphic interval where many cores showed two distinct layers. Preservation of a single sand layer suggests that sand 2 was not deposited or that it eroded and removed sand layer 3. A few examples of the deposit contained mud clasts and detrital organic debris. In some cores the base of the deposit consisted of coarser sand than the finer sand above. The sorting (generally fine grain size) and quartz-rich composition of sand layer 2 in addition to the presence of 85-percent rounded augite grains (core CANB43B; Table 2) suggest a beach source.

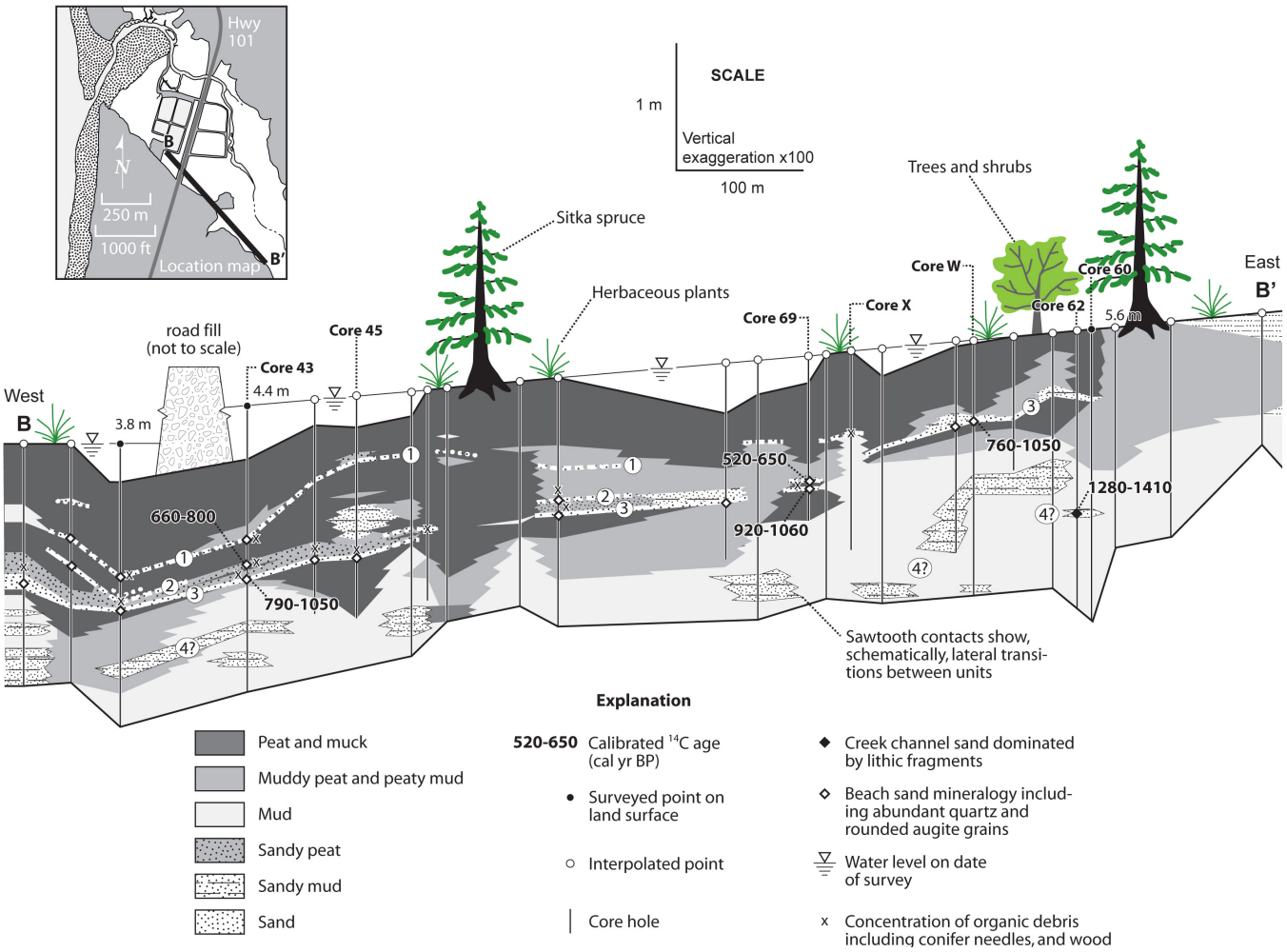


**Figure 8.** Stratigraphic profile B-B′ showing four sand layers along the southeastern margin of the lower Ecola Creek valley.

On the basis of field observations in cores within 1.6 km of the creek mouth along the southeastern margin of the valley, sand layer 3 thins in a landward direction, similarly to the overlying sand sheets (Figure 6; Figure 8). Also, like sand layers 1 and 2, the deposit is absent in cores along the central axis of the valley (Figure 6). Usually a sharp contact separates sand 3 from underlying peat or muddy peat rich in woody debris that probably formed in a wet forested lowland (Figure 12). In cores from Pompey Marsh, the sand layer consists of coarser grains at the base and includes ripped-up clasts of mud and peat. Overall, the deposit is well sorted and fine grained and consists of quartz-rich sand (Figures 12–14). More than one normally graded bed and capping layers of organic debris were observed in some deposits. About 80 percent of augite grains separated from two samples of sand 3 were rounded, similar to the percentage of rounded grains observed in modern beach sand at the end of 2nd Street (Figure 15; Table 2).

Field teams tracked sand layer 4 in sediment cores beneath the Pompey Marsh and for over 2.2 km along the central axis of the valley (Figures 6 and 9). Sand 4 was less frequently observed in cores along the southeastern valley margin (Figure 8), unlike younger sand layers that commonly were preserved along the valley margin. In contrast to sands 1–3, sand 4 is chaotically distributed and does not exhibit a clear landward-thinning trend. The sandy deposit usually interrupts sparsely rooted, inorganic mud (silt and clay) at a depth 1 to 1.5 m below the surface that was probably deposited on an ancestral floodplain of the creek or in a shallow

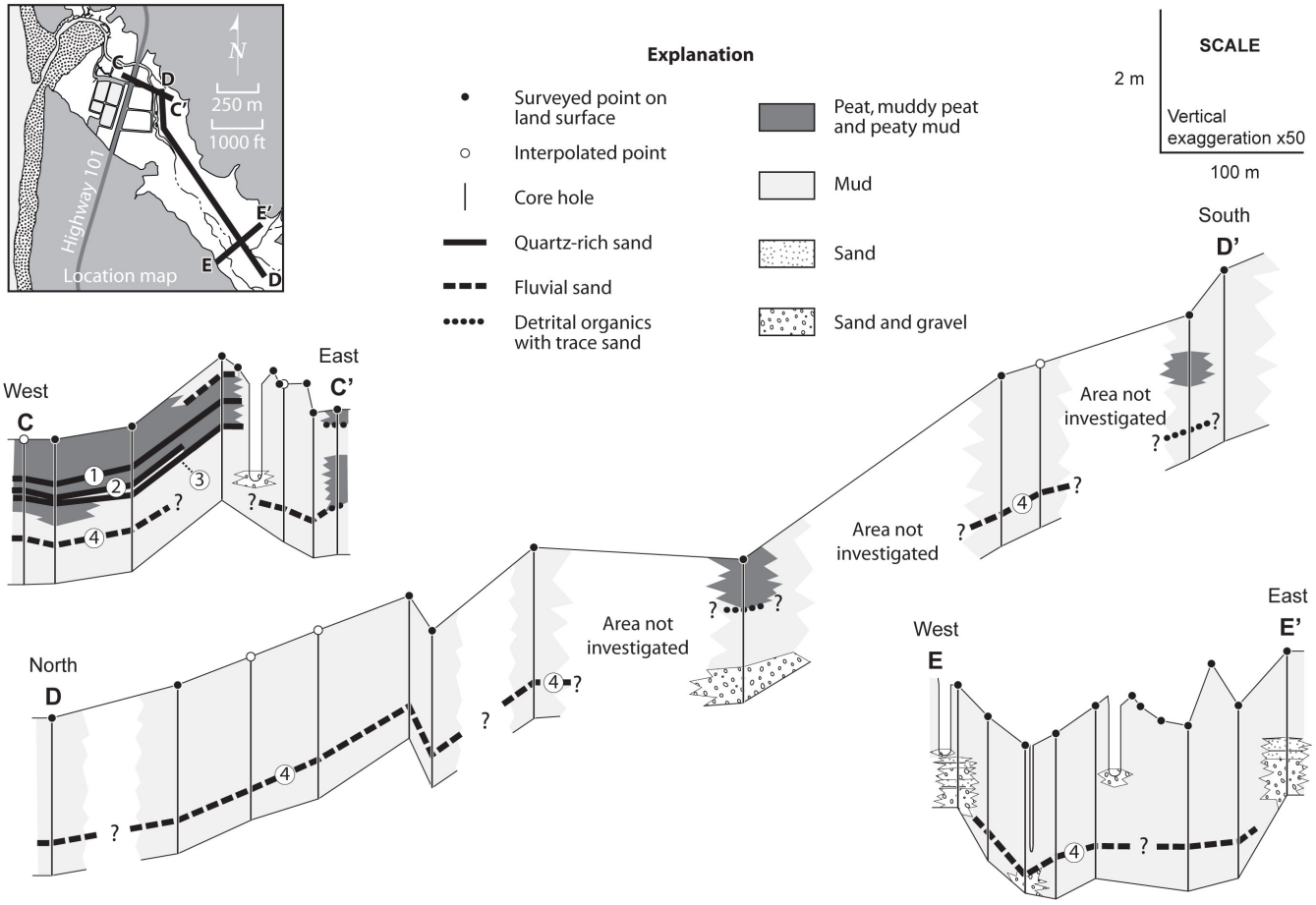


**Figure 9.** Simplified stratigraphic profiles showing sand layers correlated in cores perpendicular to profiles C-C′ and E-E′ and along the axis of profile D–D′ the lower Ecola Creek valley.

lagoon. Although some lower contacts are sharp, most are gradual in nature. The typically muddy, massive deposits contained no rip-up clasts. In some sediment cores, sand 4 was similar to sandy deposits observed at greater depths, so for the purposes of this study, sand layer 4 usually represents the first sandy layer encountered below sand 3. From field examination, sand 4 consists of abundant angular basaltic rock fragments in a silty matrix with common mica and, by comparison with beach sand, fewer quartz grains (Figure 16). In addition, samples of the deposit share grain size and mineralogy characteristics of sand found in the active channel of Ecola Creek. For example, samples from sand 4 and the creek channel show moderate sorting (higher standard deviation normalized by mean grain size) compared with beach sand and the samples feature predominantly (73 to 95 percent) angular augite grains (Figure 17; Table 2).

Rare and discontinuous younger sand lamina occurred in some sediment cores, particularly at sites located west of Highway 101. Because they were uncommon and very thin (much thinner than 0.1 in), these deposits were not sampled and analyzed to the equivalent level of detail used to characterize the more continuous and much more extensive sand layers described above. Field examination identified a mixture of quartz and lithic grains in the lamina, which suggests a mixture of beach and creek sources. Despite their limited continuity and ephemeral habit, the lamina likely record deposition by historical creek floods (e.g., 1939 and 1967) or the 1964 Alaska tsunami.

## Inferred environmental history from stratigraphy and fossil diatoms

The stratigraphy below the lower floodplain and estuary of Ecola Creek records the gradual shoaling of a drowned stream valley over several millennia. Infilling of the valley was probably controlled by a combination of factors, including rising sea level, the migration of barrier dunes, and colonization by wetland vegetation. The environmental history is inferred from a thick stratigraphic sequence of inorganic river mud overlain by 1 to 1.5 m of peat dominated by freshwater marsh diatom assemblages (Figure 18).

Changes in freshwater diatom assemblages imply a gradual shift in environment through time from diatoms that favor riverine conditions to taxa that prefer persistently wet marshes. Freshwater diatoms were most prevalent in 12 samples from core 43 (Appendix A, Table A1), located near the eastern embankment of Highway 101 (Figure 5). Diatom concentrations in

**Table 2.** Mineralogy and mean grain size data for sand deposits in the lower Ecola Creek valley.

| Sample Location | Depth Interval (cm) | Material Sampled | Mean Grain Size (mm) | Normalized Standard Deviation* | Percent Rounded Augite Grains | Percent Angular Augite Grains | Interpreted Sand Source |
|---|---|---|---|---|---|---|---|
| 2nd St. Beach | 0-5 | beach sand | 0.211 | 0.142 | 83 | 17 | beach |
| Ecola Creek | 0-5 | creek sand | 0.293 | 0.463 | 9 | 91 | creek |
| CANB43B | 52 | sand layer 1 | 0.165 | 0.207 | 59 | 41 | mixed |
| CANB43B | 82-83 | sand layer 2 | 0.195 | 0.179 | 85 | 15 | beach |
| CANB43B | 86-87 | sand layer 3 | 0.199 | 0.175 | 81 | 19 | beach |
| CANB-W | 62-63 | sand layer 3 | 0.188 | 0.175 | 77 | 23 | beach |
| CANB5 | 157-158 | sand layer 4 | 0.185 | 0.336 | 61 | 39 | mixed |
| CANB26 | 123-127 | sand layer 4 | 0.201 | 0.184 | 79 | 21 | beach |
| CANB33 | 180-184 | sand layer 4 | 0.138 | 0.317 | 27 | 73 | creek |
| CANB40 | 148-152 | sand layer 4 | 0.133 | 0.324 | 19 | 81 | creek |
| CANB42 | 71-74 | unidentified sand layer | 0.104 | 0.302 | 8 | 92 | creek |
| CANB58† | 174-177 | sand layer 4 | 0.173 | 0.434 | 20 | 80 | creek |
| CANB60 | 146-148 | sand layer 4 | 0.145 | 0.242 | 8 | 92 | creek |
| CANB62† | 135-138 | sand layer 4 | 0.126 | 0.258 | 10 | 90 | creek |
| CANB66 | 185-195 | sand layer 4 | 0.197 | 0.394 | 14 | 86 | creek |
| CANB68 | 179-182 | sand layer 4 | 0.168 | 0.303 | 21 | 79 | creek |
| CANB72 | 179-182 | sand layer 4 | 0.153 | 0.338 | 18 | 82 | creek |
| CANB74 | 100-101 | channel sand | 0.18 | 0.422 | 7 | 93 | creek |
| CANB74 | 135-140 | channel sand | >0.3 | nd | 9 | 91 | creek |
| CANB74† | 160-162 | channel sand | >0.5 | nd | 13 | 87 | creek |
| CANB78 | 190-200 | sand layer 4 | 0.118 | 0.265 | 13 | 87 | creek |
| CANB79† | 162-163 | sand layer 4 | 0.225 | 0.372 | 12 | 88 | creek |
| CANB79 | 166-167 | sand layer 4 | 0.21 | 0.441 | 15 | 85 | creek |
| CANB79 | 171-172 | sand layer 4 | 0.17 | 0.421 | 9 | 91 | creek |
| CANB80 | 190-193 | sand layer 4 | 0.13 | 0.302 | 5 | 95 | creek |
| CANB84 | 161-162 | sand layer 4 | 0.107 | 0.377 | 6 | 94 | creek |

*Standard deviation of 25 grain size measurements normalized by the mean grain size.
†Fewer than 100 augite grains examined.


**Figure 10.** Quartz-rich, fine-grained, well-sorted sand characterizes sand layer 1 in Pompey Marsh. Scale is in centimeters. Top of core is to the right of the photo.


**Figure 11.** In Pompey Marsh, sand layers 2 and 3 are separated by a mud deposit that suggests a change in the depositional environment of the marsh. Scale is in centimeters. Top of core is to the right of the photo.

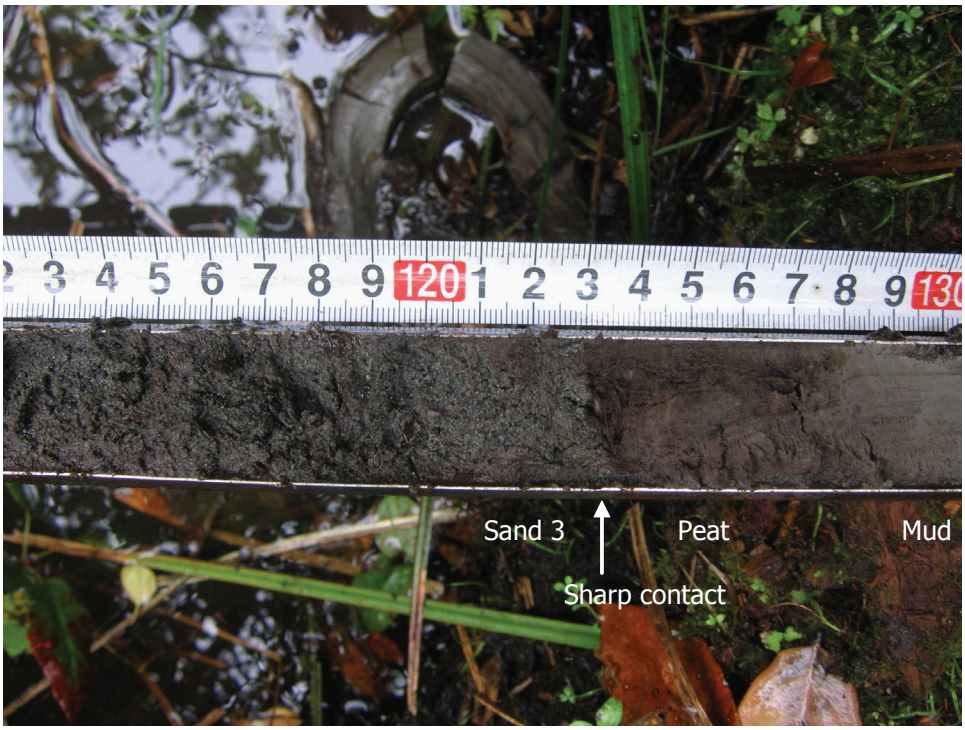


**Figure 12.** Sand layer 3, more than 10 cm thick, overlies peat rich soil of a former spruce swamp as observed in core CANB-35, located 2,460 ft (750 m) from the mouth of Ecola Creek. The sharp contact between peat and sand is about 4 ft (1.23 m) below the surface. Scale is in centimeters. Top of core is to the left.


**Figure 13.** Sand layer 3 appears as a much thinner (< 3/8 inch or < 1 cm) in core CANB-69 located 4,260 ft (1,300 m) up the valley. Forest litter and woody debris are concentrated above the sand deposit. Scale is in centimeters. Top of core is to the left.

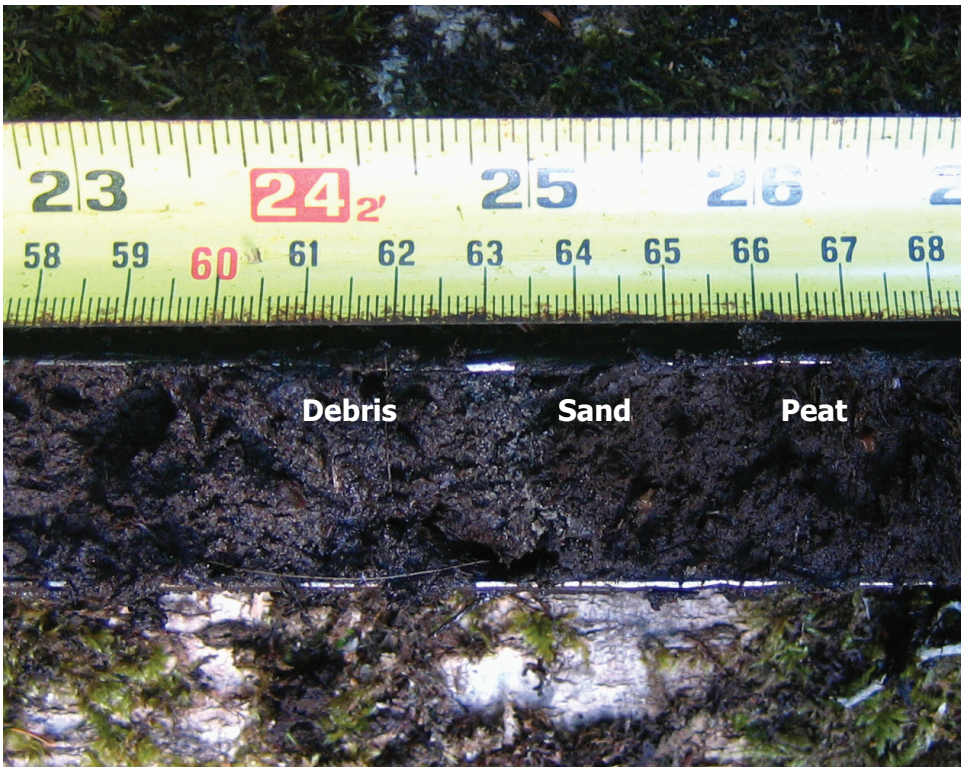


**Figure 14.** Only a trace of clean, fine-grained, quartz-rich sand is visible in core CANB-W, located 4,760 ft (1,450 m) up-valley from the creek mouth. Forest debris mixed with sand overlying sand layer 3 was sampled for radiocarbon dating. Scale is in inches (top) and centimeters (bottom). Top of core is to the left.

the samples ranged from 10,000 to 100,000 per cubic centimeter of sediment (Appendix A). The various diatom species were organized into four assemblages that reflect different ecological conditions on the basis of knowledge of modern habitats from California to Alaska. Three freshwater assemblages may distinguish between periods of persistently wet marsh conditions versus drier periods when marshes were drained or when the creek strongly influenced the site as inferred from taxa that prefer to live attached to aquatic plants along riverbanks. The fourth assemblage consists of brackish-marine diatoms subdivided into two groups: (1) Quaternary taxa found in modern coastal environments and (2) taxa represented in Tertiary deposits as well as modern environments (Quaternary-Tertiary diatoms). Extinct taxa present only in Tertiary deposits were not observed.

Before peat-forming wetland vegetation filled much of the Ecola Creek lowlands, the lower valley where much of Cannon Beach exists today may have been filled by a shallow, freshwater lagoon. Inorganic mud (silt and clay) encountered below 1 to 1.5 m in most sediment cores from valley sites and a predominance of freshwater diatoms (e.g., *Diadesmis contenta*) that prefer to live in flowing water, bogs, and lakes (Figure 18) imply a lagoonlike environment. Several freshwater coastal lagoons in Humboldt County, northern California, including Big Lagoon and Stone Lagoon, provide possible modern analogs of the prehistoric conditions at Cannon Beach. Narrow barrier sand spits that enclose these shallow coastal water bodies are periodically breached when the water surface reaches sufficient elevation above mean sea level to overtop the spit and drain the lagoon (Kraus and others, 2002). Ecola Creek, if impounded behind a barrier spit that extended across the present mouth of the creek, may have formed a similar lagoonlike environment that was seasonally or semi-annually separated from the ocean.

One to 1.5 m of peat deposited above the mud contains diatom assemblages from freshwater marsh environments that suggest the spread of wetland vegetation and the demise of the lagoon. For example, fossil

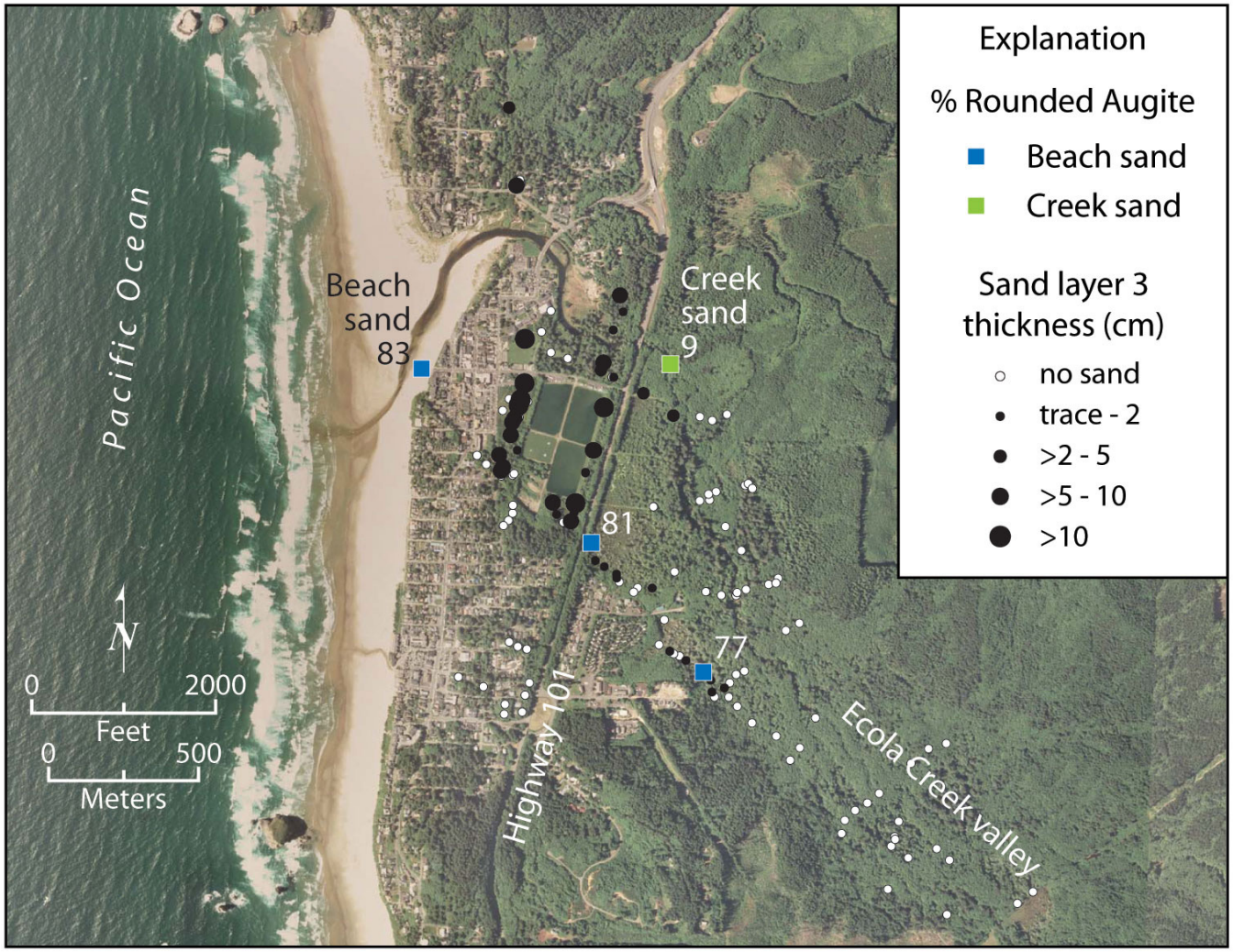


**Figure 15.** Abundant rounded augite grains occur in sand layer 3 on the basis of on heavy mineral analyses of samples from cores CANB-43B (81 percent) and CANB-W (77 percent) (Table 2). A similarly high percentage of rounded augite grains determined for samples of modern beach sand (83 percent) suggests a beach source for sand layer 3. In contrast, the sediment sample from the active channel of Ecola Creek (shown in green) contains far fewer rounded augite grains (9 percent).

species of *Pinnularia viridis* become more common in peat samples closer to the surface, implying a shift to persistently wet freshwater marsh conditions (Figure 18; Appendix A). Large pieces of woody debris impeded coring through this peat at many sites, suggesting the presence of buried stumps and logs. This wood is probably the rooted remains of Sitka spruce trees that thrived in wet bogs with perennial standing water. Today, saturated spruce bogs prevail along the southeastern margin of the valley (Figure 5).

Before extensive diking and levees isolated the wetland from the estuary, Pompey Marsh and the sloughs that dissected it were probably inundated periodically by high tides. Support for this assertion comes from historical accounts of winter storms coupled with high tides that commonly flooded Cannon Beach prior to the construction of a flood-control levee in 1970 (O'Donnell, 1996). Brackish tidal water probably rarely reached east of Highway 101. Today, salinity measurements indicate freshwater conditions in Pompey Marsh. Levees and a tide gate now separate the marsh from the river and protect Cannon Beach from storm floods and high tides.

The presence of rare but measurable brackish-marine diatoms in samples of peat, mud, and sand from core 43 indicates coastal processes that mixed marine and fresh


**Figure 16.** In contrast to the other sand layers in the Ecola Creek valley, sand layer 4 (core 73) consists of sandy mud with abundant volcanic rock fragments derived from the creek channel. Scale is in inches (top) and centimeters (bottom). Top of core is to the left.

water in the lower Ecola Creek valley. Very low abundances in nonsand samples range from 2 to 6 percent (Figure 18). Processes capable of introducing marine diatoms into freshwater wetlands along the coast include high spring tides, elevated ocean levels caused by storm surges and large waves, and wind.

Brackish-marine diatoms were more abundant in the sand layers. The highest relative abundances (21 to 22%) in sand layers 2 and 3 (Figure 18) suggest unusual ocean currents with velocities sufficient to transport beach and dune sand into the wetland. Particularly prominent in samples from sand layers 2 and 3 is *Fragilaria schulzii*, a coastal species widely distributed in North America, that lives in the nearshore marine environment attached to sand grains (Krammer and Lange-Bertalot, 1991; Witkowski and others, 2000). Less conclusive evidence for a marine origin is provided by the other sand layers, which contain fewer brackish-marine diatoms (Figure 18). Brackish-marine species comprise 8% of the species identified in a sample from a sand layer within 0.01 m below sand 3 (Figure 18) and suggest an influx of marine water. However, species adapted to river environments dominate the sample (Appendix A), suggesting the creek supplied the sand. Sand 1 contained no brackish marine diatoms. In some samples containing brackish-marine diatoms a very small component (< 3%) includes species present in the Tertiary Astoria mudstone that comprises much of the bedrock of the Ecola Creek valley (Figure 18). The presence of these species in some samples suggests the possibility that erosion and reworking of mudstone may represent a minor contribution to some deposits.

Additional data from diatom analyses of samples of sand layer 4 provide ambiguous evidence for the source of the oldest sand deposit (Table A2). Schlichting (this study) examined sparsely preserved and fragmented diatoms in samples of sand 4 in cores from 11 sites. In contrast to the abundant diatoms preserved in samples from core 43 (> 10,000 per cubic centimeter of sediment), samples of sand 4 contained only a few tens of intact specimens and multiple fragments of broken diatoms. Most samples with fewer than 100 diatoms provide unreliable data that may not represent the environmental conditions (E. Hemphill-Haley, personal communication, 2006). More surprising were the extremely low abundances of freshwater taxa compared

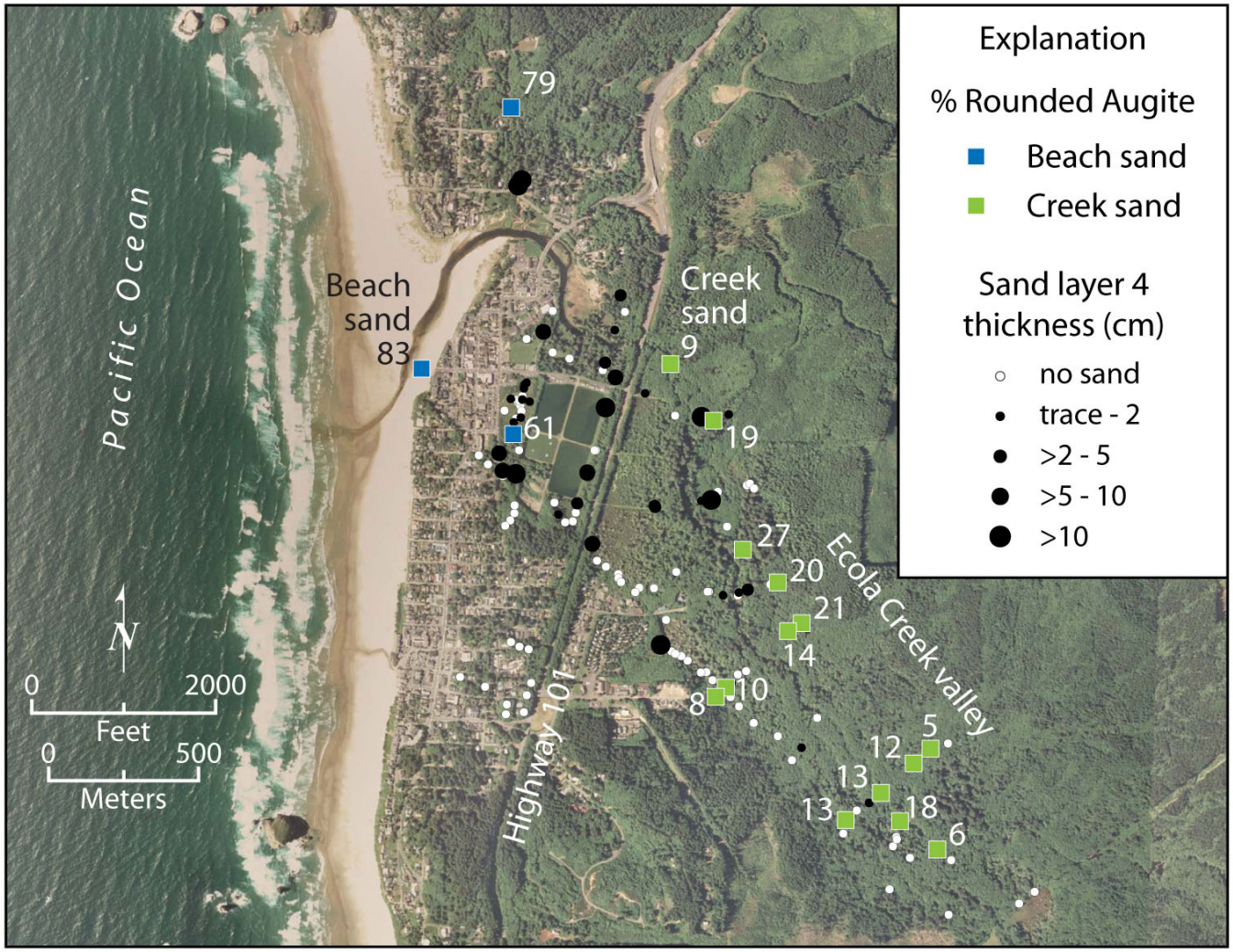


**Figure 17.** Most samples of sand layer 4 contain far fewer rounded augite grains compared with sand layer 3 and appear to reflect a similar composition to sediment in the active channel of Ecola Creek. East of U.S. Highway 101 samples of sand 4 contain 5- to 27-percent rounded augite grains compared with 9-percent observed in a modern sample of sand from Ecola Creek. Two exceptions to this observation include sand samples with 61- and 79-percent rounded augite grains from two cores located west of the highway, CANB-5 and CANB-26, respectively. The results suggest that sand layer 4 may represent two distinct deposits that reflect different depositional processes.

to the overwhelming dominance of freshwater species in samples from core 43. In samples of sand 4, the dominant intact valves in most samples are large, hardy marine species that readily survive reworking. The abundance of broken valves and preferential preservation of large robust forms more resistant to mechanical breakdown suggest the processing technique may have biased the sample by destroying most of the more delicate and fragile freshwater taxa. Among the marine diatoms preserved, the overwhelming majority belong to the Quaternary-Tertiary group. Prevalence of species from this group in sand 4 suggests a primary component of the sand and mud comes from reworking of eroded Astoria Formation mudstone in the upper watershed. However, a handful of modern marine species identified in one sample complicate a simple explanation. The presence of three valves of a modern marine planktonic diatom (*Thalassiosira pacifica*) among a few other modern marine species suggests minor mixing of marine water in a restricted estuary, possibly in a lagoonlike environment periodically breached during heavy winter storms. Alternatively, the few modern marine taxa identified may have been blown in by the wind or borne on the webbed feet of sea birds.

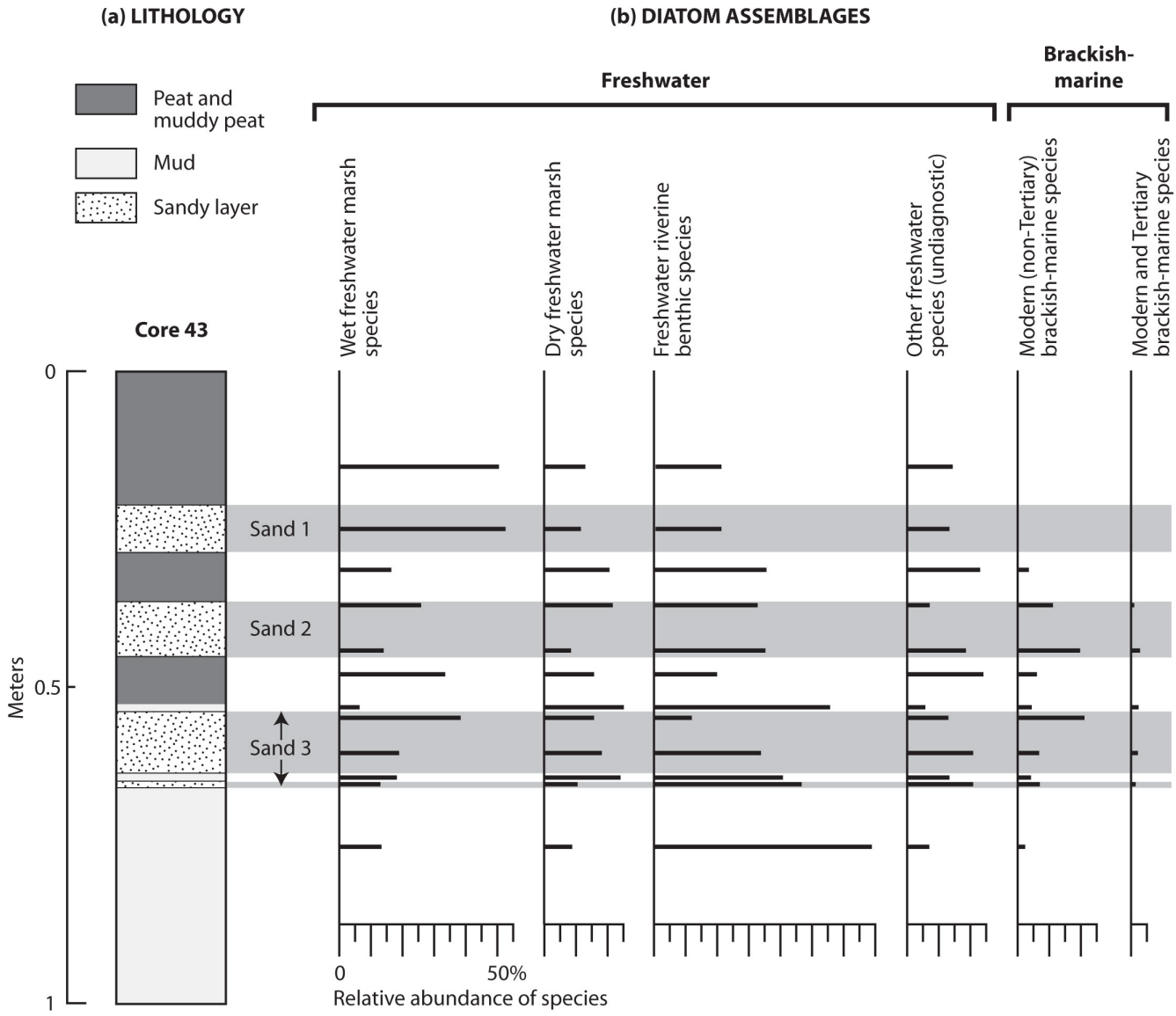


**Figure 18.** (a) Stratigraphy and (b) comparison of fossil diatom assemblages of deposits beneath the lower Ecola Creek valley. Field site location (core 43) is shown in Figure 5 and in profile B-B′ (Figure 8). Freshwater taxa are organized into four ecological groups discussed in the text. Brackish-marine taxa are grouped by their possible presence or absence in Tertiary Astoria Formation mudstone prevalent in the watershed.

## Ages of sand layers

AMS radiocarbon dates on detrital plant fossils, calibrated to account for temporal fluctuations in the concentration of atmospheric $^{14}C$ (Stuiver and Reimer, 1993; Reimer and others, 2004), estimate the times of sand deposition (Table 3). Intermixed and deposited with the sand, the fossils analyzed include conifer needles from Sitka spruce (*S. sitchensis*) and western hemlock (*Tsuga heterophylla*) trees, moss fronds and seeds of sedges (e.g., *Carex spp*.), and other herbaceous marsh plants. Because the plant material is detrital and likely died decades to years before the sand layers were deposited, age ranges provide maximum constraints on the actual date of deposition. Given these uncertainties and standard errors incorporated in the dating technique, the estimates are expressed by convention as age ranges in calibrated years before 1950 (cal yr B.P.) and span as few as 70 to as many as 280 years. The age ranges for all four sand layers correspond well with regional chronologies of Cascadia earthquakes and tsunamis documented for sites in southwestern Washington and Oregon and with offshore turbidite deposits that record margin-wide shaking (Figure 19).

A single analysis on material from the youngest sand layer in Pompey Marsh (Figure 7) constrained by European contact in 1806 limit the time of deposition for sand layer 1 to between 1680 and about 1800 (144 to 270 cal yr B.P.; Table 3). Lewis and Clark reported no sign of a recent earthquake and tsunami in 1806 when their party reached Ecola Creek in search of whale oil and blubber (O'Donnell, 1996), and reports of tsunamis in written history after the expedition are not known. Therefore, if sand 1 records inundation by a Cascadia tsunami, sand 1 probably dates to January 1700, the time of the most recent tsunami generated by the subduction zone (Satake and others, 1996). Gallaway and others (1992) dated bulk peat within several inches below the same sand deposit, but the much older date (310 to 510 cal yr B.P.) was probably contaminated by plant material that had accumulated over several hundred years prior to the event that deposited the sand. Ubiquitous evidence and more accurate age estimates for the 1700 Cascadia earthquake have been reported at coastal sites north and south of Cannon Beach (Figure 19).

Two dates on material sampled from separate sites (cores 43 and 69; Figure 8) provide a broad age estimate of 520 to 800 cal yr B.P. (Table 3) for the origin of sand layer 2. Individually, the dates do not overlap and meet criteria that define a statistical difference at the 95% level. Without further dating, no other information is available to evaluate the most accurate age; thus the dates were combined into a single range that spans 280 years.

Sand 2 correlates in time with possible earthquake evidence at Netarts Bay (OF-II/2MT) and with one of two earthquake-triggered turbidites (T2 or T3; Figure 19). It also overlaps ages of Cascadia tsunami evidence reported at Discovery Bay, the Naselle River, and Johns River in Washington (Williams and others, 2005; Shennan and others, 1996) and at Tofino, on Vancouver Island, British Columbia (Clague and others, 2000).

The pooled mean age (910 to 980 cal yr B.P.) of three statistically indistinguishable $^{14}C$ dates estimates the deposition time of sand layer 3 (Figure 8; Table 3). Similar dates on detrital samples from three separate samples of the deposit at three separate sites independently confirms stratigraphic correlations derived from field observations (Figure 8). Although still a maximum date, the age range is the most precise among estimates of the four sand layers and spans only 70 years. The age of sand 3 corresponds to the time of a Cascadia earthquake and tsunami about 1,000 years ago recorded regionally at sites to the north and south of Cannon Beach (Figure 19).

The muddy sand layer 4 mapped beneath the floodplain of the lower Ecola Creek valley (Figure 9) dates to 1,280 to 1,410 cal yr B.P. from a single calibrated age on a Sitka spruce cone sampled from core 62 (Figure 8; Table 3) located far from the creek mouth. Because stratigraphic correlations for sand 4 are less conclusive and because the date is based on a single analysis, this age range may not be an accurate estimate for the deposit mapped as sand 4 beneath the Pompey Marsh and at other sites near the mouth of the creek. The age range for sand 4 predates the more precise date of event U in southeastern Washington (Atwater and Hemphill-Haley, 1997; Atwater and others, 2003) but overlaps the lower ranges of ages for events reported in Oregon south of Cannon Beach (Figure 19).

**Table 3.** Calibrated age estimates of sand sheets in the lower Ecola Creek valley derived from accelerator mass spectrometry (AMS) radiocarbon dates on detrital macrofossils.

| Sand layer no.* | $^{14}$C lab number# | Core Number† | Sample depth in core (m) | Material dated | $\delta^{13}$C (‰) | Lab-reported age ($^{14}$C yr BP at 1σ)§ | Calibrated age (cal yr BP at 2σ)** | Relative area under probability distribution## | Preferred age estimate for sand layer†† |
|---|---|---|---|---|---|---|---|---|---|
| 1 | 228613 | POMP-1 | 0.46 | needles, moss, seeds | –27.2 | 90 ± 40 | 12–148<br>187–199<br>211–269 | 0.69<br>0.02<br>0.27 | 144–270§§ |
| 2 | 219693 | CANB-69 | 0.96 | moss | –28.0 | 570 ± 40 | 521–570<br>580–651 | 0.40<br>0.60 | 520–800*** |
| | 230216 | CANB-43R | 1.25 | needles, moss, seeds, twig | –27.3 | 790 ± 50 | 658–795 | 0.99 | |
| 3 | 220572 | CANB-W | 0.62 | conifer needles | n.d. | 990 ± 60 | 765–1004<br>1,030–1052 | 0.97<br>0.03 | 910–980### |
| | 230217 | CANB-43R | 1.39 | needles, moss, seeds, twig | –30.0 | 1,000 ± 50 | 788–989<br>1, | 0.97<br>0.03 | |
| | 219694 | CANB-69 | 1.04 | moss | –24.3 | 1,050 ± 40 | 916–1058 | 1 | |
| 4 | 220573 | CANB-62 | 1.35 | conifer cone | –24.5 | 1,430 ± 50 | 1,276–1411 | 1 | 1,280–1,410 |

* Radiocarbon age data grouped by sand sheet number determined by stratigraphic correlation. Sand sheet numbers increase with age.

\# All samples submitted to Beta Analytic, Inc., Miami, Florida, for $^{14}$C dating using AMS techniques.

† Core number designates locality; specific core identified by letter. Localities are POMP, Pompey Marsh; CANB, Cannon Beach.

§ Conventional ages reported by radiocarbon laboratory are based on the Libby half life (5,570 years) for $^{14}$C.

** Calibrated age ranges before AD 1950 are reported to the nearest year using the computer program Calib rev. 5.0.1 (Stuiver and Reimer, 1993) and the IntCal04 calibration data set of Reimer and others (2004) with a lab error multiplier of 1.0 and reported to 2σ.

## Age intervals with less than 0.01 relative area under the distribution are not shown.

†† Age ranges are rounded to the nearest decade except for historical constraints on the estimate for sand layer 1.

§§ Upper bound of age range is constrained by the year 1806, when Lewis and Clark reached Ecola Creek and written history began in coastal Oregon.

*** Age range represents the sum of probabilities for both $^{14}$C ages for sand layer 2. The two samples meet a Xi-square test that shows a statistical difference at the 95% level.

### Age range represents 97% of the relative area of the calibrated age distribution for the pooled mean age of the three $^{14}$C dates for sand layer 3. The three ages are indistinguishable based on a Xi-square test for statistical difference at the 95% level.

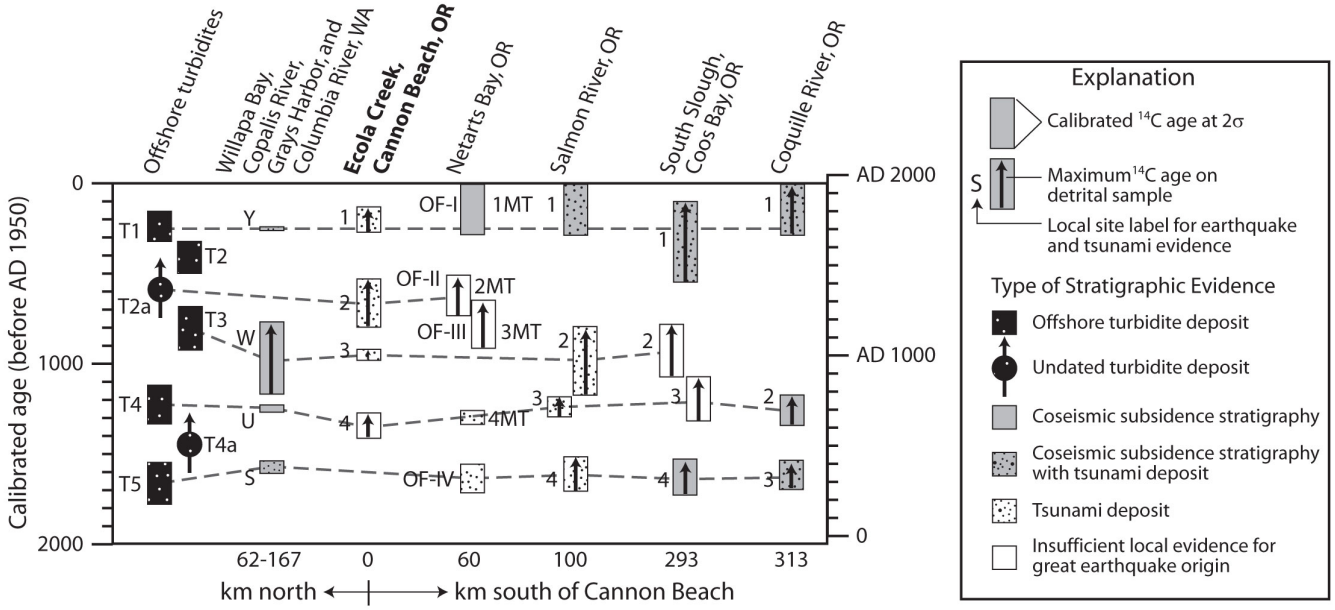


**Figure 19.** Comparison of calibrated $^{14}C$ ages and coastal evidence for great Cascadia earthquakes and tsunamis over the last two millennia at six sites in southwestern Washington and northwestern Oregon (modified from Nelson and others, 2004). Black rectangles represent ages for offshore turbidite deposits inferred to record strong shaking during prehistoric Cascadia earthquakes (from supplementary Table 2 of Goldfinger and others, 2008). Arrows indicate maximum limiting $^{14}C$ ages based on dates of detrital plant fossils. Ages for evidence at sites in southwestern Washington are from Atwater and others (2003). Ages from coastal sites in Oregon are from Ecola Creek (this study), Netarts Bay (Darienzo and others, 1994; Nelson and others, 1995; Shennan and others, 1996), Salmon River (Nelson and others, 1995, 2004), South Slough, Coos Bay (Nelson and others, 1996, 1998), and the Coquille River estuary (Witter and others, 2003). Local evidence for earthquake-related subsidence is lacking for one or more stratigraphic contacts at Ecola Creek, Netarts Bay and Coos Bay (e.g., Shennan and others, 1996).

## HISTORY OF TSUNAMIS AND FLOODS AT CANNON BEACH, OREGON

Several processes are capable of depositing layers of sand in the floodplain and wetlands of the lower Ecola Creek valley, including inundation by high tides especially during extreme winter storms, tsunamis from both local and distant earthquakes, and severe flooding by Ecola Creek. By considering multiple criteria that favor a tsunami origin (Table 4), I evaluate the likely origin of each sand sheet and, where possible, preclude possible alternative explanations. Three sand sheets meet all but one or two of the criteria for deposition by a local Cascadia tsunami. The distribution and extent of the sand layers provide minimum constraints on the inundation and runup of prehistoric Cascadia tsunamis that hit Cannon Beach in the last 1,000 years. Comparisons between the extent of the tsunami deposits and modeling results helps establish the validity of numerical tsunami simulations used to delineate tsunami hazard zones and guides emergency planners in the design of safe evacuation routes.

### Tsunamis and alternative explanations for sand deposits

The three youngest, widespread sand deposits (sand layers 1, 2, and 3) mapped beneath the lower Ecola Creek valley meet all but one or two of the criteria for deposits of tsunamis produced by prehistoric Cascadia subduction zone earthquakes (Table 4). The sand layers were not deposited by a flood of Ecola Creek because each possesses characteristics of a beach or marine source. Each sand layer shares the attributes of modern sand from the beach and dunes that front Cannon Beach, including an abundance of well-sorted, fine-textured quartz and rounded augite grains (Table 2). Two

**Table 4.** Summary of evidence for sand layers deposited in the lower Ecola Creek valley that satisfy criteria for a tsunami origin.

| | Sand Layer | | | |
|---|---|---|---|---|
| **Type of Evidence** | **1** | **2** | **3** | **4** |
| Deposit has attributes of beach sand* | ✓ | ✓ | ✓ | no |
| Modern brackish-marine diatom present | no | ✓ | ✓ | **I**† |
| Deposit thins/grain size fines landward | ✓ | ✓ | ✓ | no |
| Normally graded beds observed | ✓ | ✓ | ✓ | no |
| Rip-up clasts present in deposit | ✓ | ✓ | ✓ | no |
| Sharp or eroded lower contact | ✓ | ✓ | ✓ | ✓ |
| Organic debris present at top of deposit | ✓ | ✓ | ✓ | ✓ |
| Extent of deposit (km)§ | 1.45 | 1.40 | 1.60 | 2.20 |
| Deposit is coincident with earthquake-subsided soil | **I** | no | **I** | no |
| Age overlaps with evidence for regional Cascadia event# | ✓ | ✓ | ✓ | ✓ |

Note: checkmark (✓) indicates the evidence was observed at multiple sites; **I**, data are insufficient to provide conclusive evidence; "no" indicates the absence of evidence.

* Beach sand component interpreted from sand mineralogy and grain size data listed in Table 2.

† Rare fossil marine diatoms identified in sand layer 4 were also present in silty sediment above and below the sand layer. Sand sheet distribution shown in Figure 6 and other physical attributes of sand layer 4 suggest a river source and that fossil marine diatoms were likely reworked from Tertiary Astoria Formation marine mudstone present in the upper watershed of Ecola Creek.

§ Landward extent of deposit measured from mouth of Ecola Creek to core site farthest inland where sand sheet was observed. Only tsunamis or high stream flow could explain such widespread deposits in the lower valley, ruling out storm waves superimposed on extreme ocean levels as an alternative explanation.

# Correlations are based on regional geologic records of Cascadia earthquakes and tsunamis shown in Figure 16.

of the deposits (sands 2 and 3) contain elevated numbers of brackish-marine diatoms (Figure 18), including one diagnostic species, *Fragilaria schulzii*, that lives on sand grains in nearshore marine environments (Appendix A). Observations that the deposits become thinner (Figure 6) and that the sand grain size becomes measurably finer in a landward direction (sand 3 samples, Table 2) also suggest that marine surges, not high stream flow of Ecola Creek, deposited the sands. The sand layers exhibit other features commonly observed in tsunami deposits, including normally graded beds, muddy rip-up clasts, sharp or eroded lower contacts, and organic debris capping each deposit (Table 4). All three deposits extend 1.4 to 1.6 km inland (Figure 6), far beyond the reach of ocean waves superimposed on winter storm surge as an alternative explanation. Finally, age estimates for all three sand layers overlap with inferred times of great earthquakes and tsunamis reported from other sites above the Cascadia subduction zone (Figure 19).

Little evidence was found to cast doubt on Cascadia tsunamis as the best explanation for sand layers 1, 2, and 3. However, the stratigraphy lacked conclusive evidence for earthquake-induced subsidence, a common feature associated with tsunami deposits. At most sites the sand layers separated deposits of freshwater peat, possibly reflecting that the sites were too high in elevation to respond to small (< 0.5 m) amounts of subsidence that may have accompanied the tsunami. At many coastal wetlands in Oregon, particularly salt marshes, the response is manifested as a vertical shift in environment resulting from a sudden rise in relative sea level caused by the subsidence. Possible lithologic evidence for subsidence appears as mud or muddy peat overlying sand layers 1 and 3 in a few cores from Pompey Marsh. If, near the creek mouth, the prehistoric marsh was influenced by tides, then an increase in mud content in deposits above some sand layers relative to the underlying peat could reflect a vertical shift from high salt marsh to lower intertidal conditions that would be expected if the elevation of the wetland dropped during an earthquake. However, without a comparison of the fossil diatom assemblages in the muddy deposits relative to assemblages in the peat below the sands, there are no data to suggest a rise in relative sea level caused by earthquake subsidence.

The absence of brackish-marine diatoms in a sample of sand 1 from core 43 (Figure 19) seems inconsistent with evidence at other sites that favors a marine origin for the 1700 tsunami deposit. Also, unlike the high abundance (> 80%) of rounded augite grains found in most beach sands, rounded grains amounted to just over half (59%) of the augite grains in sand 1 from core 43 (Table 2). At most other sites where sand 1 was identified, the deposit consisted of fine-grained, quartz-rich sand that in hand sample (Figure 10) appeared very similar to the texture and mineralogy of beach sand. The unexpected results for samples of sand 1 from core 43 suggest the possibility that the 1700 tsunami deposit at that site may have been contaminated by sediment related to construction of the highway road embankment or destroyed altogether.

In contrast to the youngest three sand deposits, sand layer 4 satisfies far fewer criteria consistent with tsunami origin (Table 4). The deposit lacks the attributes of beach sand, instead possessing characteristics similar to deposits in the modern creek channel (Table 2). The apparently chaotic distribution of sand 4 along the central axis of the valley, the absence of a landward-thinning deposit, no observed rip-up clasts, and a generally massive nature argue against emplacement by tsunami. Nowhere did I observe evidence of earthquake-related subsidence associated with the sand deposit. Rare cases where the lower contact of the deposit was sharp or eroded and the occasional presence of organic debris within the sand lends equivocal evidence for a tsunami origin, but other processes like river floods can also form such features. The presence of sparse marine diatoms in some samples of sand 4 suggests a marine source, but questions about the technique used to process the samples and the overall absence of freshwater species presents the possibility that the samples may be biased toward preservation of the larger, more resistant marine forms. Further evidence that discredits a marine origin is the fact that extant Tertiary species dominate (59 to 100%) the fossil marine taxa identified and suggest that a significant component of the deposit reflects reworked, redeposited material from Miocene mudstone of the Astoria Formation that underlies large areas of the watershed.

A few observations suggest that sand 4 might be a tsunami deposit: its widespread extent and an age similar to a known Cascadia earthquake and tsunami that occurred about 1,250 years ago (Figure 19). Although field mapping tracked the deposit for over 2.2 km up the valley, the furthest extent of all the sand layers identi-

fied, the extensive coverage of the deposit does not rule out flooding of the creek as an alternative hypothesis. In addition, several other lines of evidence support a creek channel rather than the beach as the likely source of sand 4: mineralogy (Table 2), distribution along the central axis of the valley (Figure 6), and massive texture and composition much like the sandy flood deposits observed in exposures of the natural creek levee and similar deposits observed in February 2007 that mantled the modern levee after a series of winter storms. The coincidence that the age of sand 4 closely predates the inferred timing of a Cascadia earthquake and tsunami is more difficult to explain.

Radiocarbon dates, often with uncertainties that span several hundred years, offer poor constraints to make definitive temporal correlations between earthquake and tsunami evidence recorded at separate sites (Nelson, 1992). If the age range for sand layer 4 (1,280-1,410 cal yr B.P.) accurately brackets the true age of the deposit, then sand 4 may reflect a flood that occurred 20 to 180 years before earthquake U, which has been precisely dated to 1,230–1,260 cal yr B.P. at sites in southwestern Washington (Atwater and others [2003] converted from the combined age for earthquake U in their Appendix 1 reported in cal yr A.D.). However, because the material dated from sand layer 4 (a single spruce cone, Table 3) died before material was deposited, the age estimate probably predates the actual time of deposition by a number of decades to perhaps more than one hundred years. So it is not unreasonable to infer that sand 4 was deposited near the time of a Cascadia earthquake and tsunami about 1,250 years ago. Why would the age of sand layer 4, if deposited during a flood of Ecola Creek, closely match the time of a Cascadia earthquake and tsunami recorded at other sites in southwestern Washington and Oregon? Possible explanations include potential hydrological changes to the system caused by earthquake-induced subsidence and greater sediment supply in the upper watershed mobilized by earthquake-triggered landslides. If subsidence during the earthquake raised relative sea level and the base level of the creek, floods of the creek may have more frequently overtopped levees and led to sand deposition on the floodplain where prior floods had deposited mostly silt. Alternatively, landslides and debris flows induced by seismic shaking could have increased the sediment supply to the creek; during high flow the sediment could have been deposited on the floodplain as a layer of massive sand rich in volcanic rock fragments and disaggregated mudstone derived from bedrock in the upper watershed.

Discontinuous sandy lamina, often no thicker than several fine sand grains, and some consisting primarily of fine quartz grains, were noted in many core descriptions and were often found at different stratigraphic depths. Several explanations can account for these thin sands interlayered with peaty deposits beneath wetlands along Ecola Creek. Sand thrown aloft by strong westerly winds during winter storms could mantle marshes with thin, discontinuous layers of fine aeolian sand. Bioturbation and liquefaction (Peterson and others, 2008) have been proposed as other reasonable explanations. However, one of two other processes probably best explains the youngest sand lamina observed at several sites in Pompey Marsh: the 1964 Alaska tsunami or the 1967 flood. In their summary of the effects of the 1964 tsunami at Cannon Beach, Lander and others (1993, p. 97) reported that "[t]he water poured down the street carrying logs, debris and sand everywhere between the buildings and littering the street." It is not unreasonable to postulate that the tsunami also left a layer of sand and debris in the wetlands adjacent to the city. Alternatively, given the historical accounts of at least 2.5 ft (0.8 m) of water in downtown Cannon Beach (O'Donnell, 1996), the 1967 flood also may have left a visible layer of sand in the geologic record. Too few traces of the youngest sand lamina and its discontinuous distribution prevent a thorough evaluation of criteria that favor a tsunami over a flood origin.

### Minimum tsunami inundation

Traces of sand and debris that define the landward limit of deposits left by prehistoric Cascadia tsunamis represent minimum estimates of the extent of inundation. Sand layers 1, 2, and 3 extend 1.4 to 1.6 km inland as measured from the beach where Ecola Creek flows into the Pacific Ocean (Figure 6). Surveys of historical tsunamis (e.g., 1998 Papua New Guinea tsunami; 2004 Indian Ocean tsunami) report that the inland limit of inundation in many cases lies within about 50 m of the extent of sand deposition (Gelfenbaum and Jaffe, 2003; B. Jaffe, personal communication, 2006). However, without direct evidence of the inland extent of the tsunami wave (e.g., scour marks, stripped vegetation, wrack lines) flooding for tens to hundreds of meters

beyond the last vestige of sand deposited by the wave cannot be ruled out.

In 1964 the Alaska tsunami destroyed the old Elk Creek bridge, flooded two city blocks, tore houses from foundations, and damaged the Highway 101 bridge (Lander and others, 1993). Various reports of the water depths during the first tsunami surge provide crude estimates of runup from which to infer the extent of inundation (Figure 4). Along the seaward side of the barrier spit and in the small valley north of the Ecola Creek outlet channel an inferred runup of 16 ft (4.9 m) (NGVD 29) was used to delineate the inundation extent. Elsewhere west of Highway 101, including the landward side of the sand spit, the 10-ft (~3-m) contour was used to approximate the extent of inundation. If the Alaska tsunami extended west of the highway, it was probably confined to the creek channel; there are no known reports of water overtopping the highway embankment.

### Minimum tsunami runup on the open coast

Field data from upland sites in Cannon Beach provided little evidence to estimate minimum open coast runup reached by prehistoric tsunamis. Shallow (< 0.5-m-deep), thin (0.03- to 0.05-m-thick), quartz-rich sand deposits were identified beneath an upland swale (core 131, Figure 5) at an elevation of 32 ft (9.8 m) (NAVD 88), but evidence for a tsunami origin is inconclusive. Repeated coring in the swale at seven sites within tens of meters of core 131 failed to identify similar sandy deposits. Because the sand deposit was found at a single site and did not appear to represent a continuous layer that extended across a significant length of the swale, competing explanations for the origin of the deposit become more credible. For instance, because the swale runs through a residential neighborhood where most of the original landscape has been extensively modified by grading for housing construction and landscaping, the swale appears to be a likely sink for local surface water runoff that could transport sandy sediment often present at construction sites and commonly used in landscaping. I observed a large pile (approximately 1 $m^3$) of beach sand in the driveway of a house directly adjacent to the swale that, if transported down slope into the swale by surface water runoff during heavy rainfall, would leave a thin deposit of beach sand similar to the deposit observed in core 131. Although historical infilling of the marsh provides the most reasonable explanation for sandy deposits found at a single upland site, the available data cannot rule out that a prehistoric tsunami deposited the sand reaching a present elevation of 32 ft (9.8 m) (NAVD 88).

Lacking upland sites that provide more conclusive limits on the runup magnitude of prehistoric Cascadia tsunamis, one can infer crude runup estimates from runup estimates for the 1964 Alaska tsunami. The 1964 tsunami did not overtop the 20- to 24-ft- (6.1- to 7.3-m-) high (NAVD 88) barrier sand ridge that fronts Cannon Beach. However, eyewitness accounts suggest runup may have reached elevations of 19 to 20 ft (5.8 to 6.1 m) (NAVD 88), nearly overtopping the crest of the barrier. Prehistoric tsunamis probably had little trouble overtopping any similar dune, if present. Considerable uncertainty in the actual elevation of the barrier sand ridge during past tsunamis precludes a precise estimate, but a minimum runup elevation of 20 ft (6.1 m) seems reasonable considering estimates of the maximum runup at Cannon Beach in 1964.

### Empirical tests of numerical tsunami simulations

Three tsunami deposits at Cannon Beach provide estimates of minimum inundation from prehistoric Cascadia tsunamis that can be used to test numerical simulations of tsunami inundation. For example, Figure 20 compares existing numerical models to the distribution of sand layer 3. The initial numerical models for this comparison used a numerical grid based on 10-m topographic data with no attempt to reconstruct the prehistoric landscape that existed when sand 3 was deposited. Model 1A used by DOGAMI (Priest and others, 1997a) to develop Oregon's tsunami hazard maps produces inundation that falls seaward of the total extent of sand layer 3 mapped in Ecola Creek valley. Much larger Cascadia tsunamis simulated using two source models developed for the Seaside, Oregon Tsunami Pilot Study (Tsunami Pilot Study Working Group, 2006; models S5 and S9 from Eric Geist, personal communication, 2006) appear to extend tens to a few hundred meters beyond the inland extent of sand layer 3. The models depicted in Figure 20 may underestimate inundation because improvements to the numerical code as the result of analytical tests predict more extensive inundation (Priest and others, 2008).

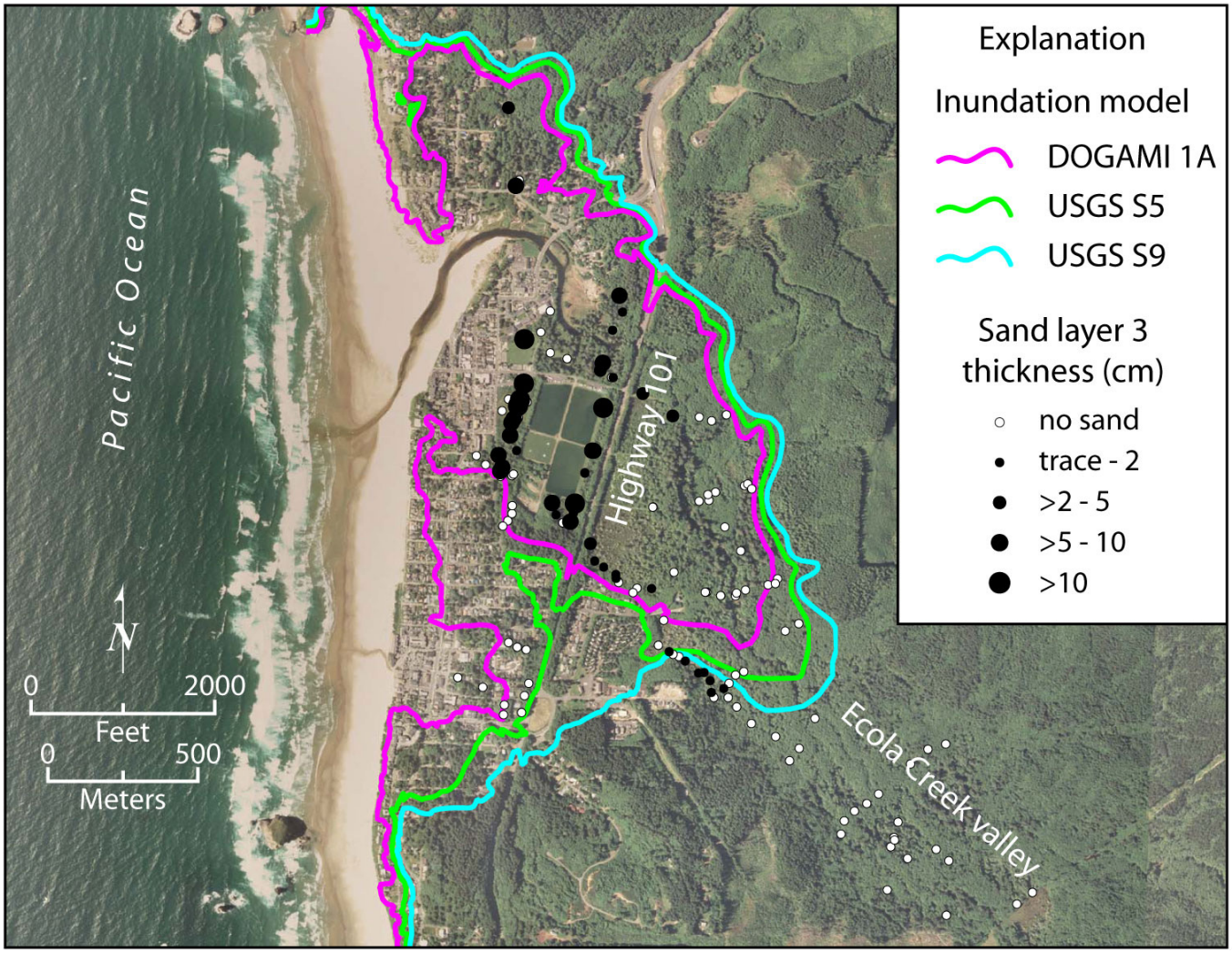


**Figure 20.** Comparison of existing numerical tsunami inundation models (DOGAMI 1A , Priest and others, 1997a; U.S. Geological Survey models S5 and S9, Eric Geist, personal communication, 2006) to distribution of sand layer 3.

Test simulations using new earthquake source models developed by Priest and others (2008) were run using a gridded digital elevation model designed to represent prehistoric topography inferred from available geologic data. The reconstructed landscape removed artificial fill, road embankments, and levees and accounted for 1,000 years of erosion of coastal bluffs (Priest and others, 2008). The model landscape also removed sediment aggradation in the lower Ecola Creek valley over the same time period and varied the presence or absence of a barrier dune to explore the possibility that the dune was an ephemeral feature in the landscape. Because the largest wave heights overtopped the dune, test results showed negligible variation (tens of meters) for the largest Cascadia tsunami simulations whether the sand barrier was present or absent. However, the presence of a barrier dune had a significant effect on the inundation for tsunamis of smaller earthquake sources compared to simulations run without the sand barrier. Simulations using the modern landscape, which includes a barrier dune, generally predicted less inundation than simulations using the prehistoric topography due to the presence of artificial fills and embankments that act as barriers to flow. The elevation of the Ecola Creek valley also appeared to have little effect on model simulations because the elevation was inferred to vary as a function of sea level rise.

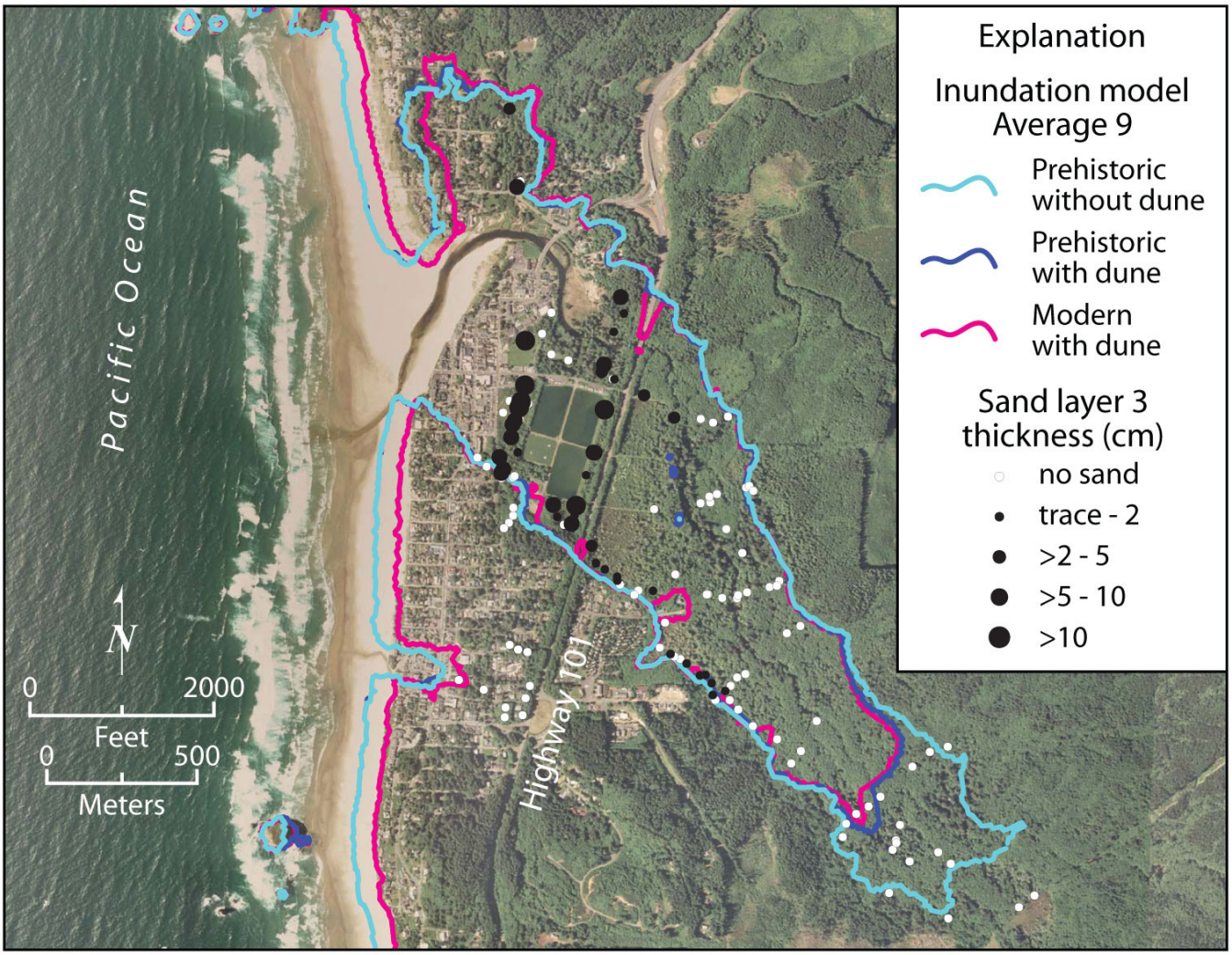


**Figure 21.** Numerical simulations for tsunami scenario "average 9" compared with the distribution of sand layer 3. Blue lines show inundation for simulations run on a prehistoric landscape. Magenta line shows inundation for the same simulation on a modern landscape.

Test simulations of Cascadia tsunami scenario "average 9" are shown in Figure 21 and are compared to the extent of sand layer 3. Sand 3 was selected as an empirical reference because it extended farther inland than any other tsunami deposit of the last 1,000 years. The simulations shown by the blue lines use a digital elevation model that represents the inferred prehistoric landscape 1,000 years ago. Both simulations exceed the mapped inland extent of sand layer 3, a tsunami deposit inferred to represent a medium-size Cascadia tsunami on the basis of correlation with offshore turbidite records (Goldfinger, 2008). Also shown in Figure 21 is a third simulation (magenta line) using the same model parameters but run with a modern digital landscape. The three simulations use the same earthquake source inputs developed by Priest and others (2008). Because deposits of prehistoric tsunamis provide a minimum constraint on inundation, both simulations run on a prehistoric landscape with and without a sand dune are consistent with the distribution of sand layer 3. Tsunami simulations that produced greater inundation would also be consistent with the geologic data because inundation meets or exceeds the landward limit of the sand deposits.

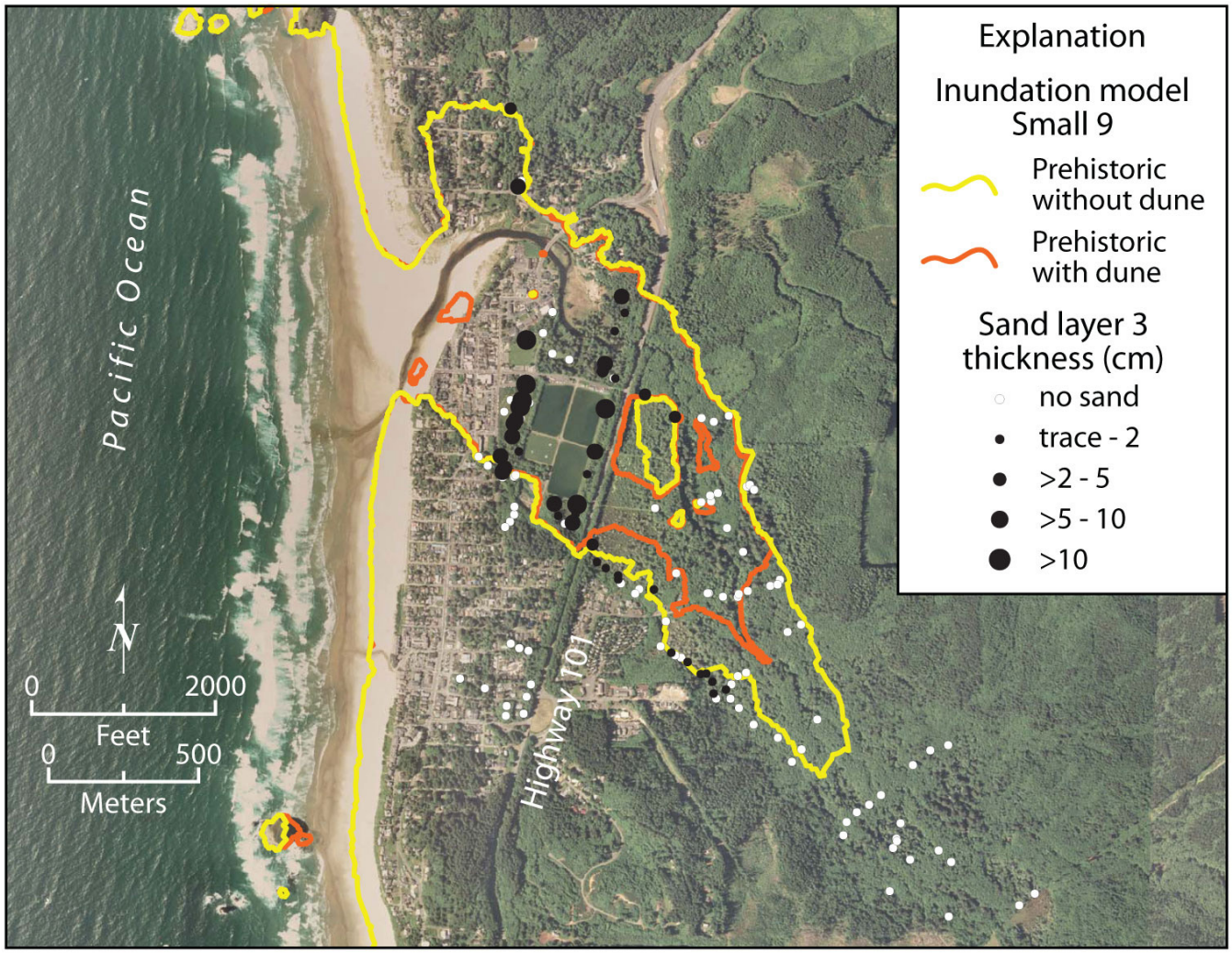


**Figure 22.** Numerical simulations for the tsunami scenario "small 9" (Priest and others, 2008) compared with the distribution of sand layer 3. Both lines show inundation for simulations using a prehistoric landscape.

Test simulations for a smaller Cascadia tsunami scenario, "small 9," also are compared with the distribution of sand layer 3 (Figure 22). Priest and others (2008) developed 26 different tsunami scenarios that ranged in size from "small" tsunamis produced by a model earthquake with 10 m of slip to the "largest" scenario produced by a giant model earthquake with 45 m of slip. Such variability in earthquake size was suggested by variability in the physical properties and recurrence intervals of offshore turbidites that record 20 Cascadia earthquakes in the last 10,000 years (Goldfinger and Morey-Ross, 2004; Goldfinger, 2008). The comparison shows that inundation for the "small 9" scenario run without a sand dune greatly exceeds the inundation for the same scenario run on a prehistoric landscape that includes a sand dune. As a result, the scenario run with a barrier dune stops far short of sand layer 3. Although the scenario run without a sand barrier inundates farther up the valley, it also falls just short of the deposit, approaching to within 70 m of the furthest extent of sand layer 3. Inundation lines for both scenarios fail to reach the inland extent of sand layer 3 and are inconsistent with empirical evidence of inundation produced by prehistoric tsunamis.

# CONCLUSIONS

Cannon Beach faces significant hazards from future distant tsunamis and local tsunamis generated by Cascadia subduction zone earthquakes. Historical accounts and geologic data provide the basis for this assessment of tsunami runup and inundation during the 1964 Alaska tsunami and for at least three prehistoric Cascadia tsunamis that flooded the lower Ecola Creek valley within the last 1,000 years. The 1964 Alaska tsunami caused considerable damage to city infrastructure as well as private property in Cannon Beach (equivalent to over $1.62 million in 2008 dollars). Eyewitness reports in newspaper stories released days after the March 27 tsunami afford credible information from which to estimate the extent of inundation and the elevation of wave runup. Maximum runup probably reached 19 to 20 ft (6.1 m) (MLLW), extrapolated from estimates of the tsunami flow depth at two sites: the Bell Harbor Motel and the Steidel residence (Table 1). The extent of inundation caused by the 1964 tsunami (Figure 4) was inferred from reports of damage to the U.S. Highway 101 bridge (Lander and others, 1993), extensive flooding of the business district of the city (Schlicker and others, 1972), and extrapolation of flow depth estimates and inferred runup using a 2-ft (0.6-m) contour map provided by the city of Cannon Beach (Figure 3).

Three additional severe tsunamis inundated Cannon Beach within the last 1,000 years and flooded the lower 1.4 to 1.6 km of the Ecola Creek valley. The minimum extents of inundation come from the mapped distribution of three sand layers, all of which satisfy eight or nine out of 10 criteria that are characteristic of tsunami deposits (Table 4). Some evidence favoring a tsunami origin includes mineralogical and sedimentological attributes of beach sand, the presence of fossil brackish-marine diatoms, a sharp or eroded lower contact, a trend where the deposit becomes thinner away from the ocean, and $^{14}C$ age estimates that are consistent with regional Cascadia earthquake and tsunami chronologies.

A fourth sand layer was probably deposited by a large flood of Ecola Creek. The relatively large size of this coastal watershed and high seasonal rainfall make Ecola Creek susceptible to flooding, and historical accounts indicate that moderate flooding has occurred several times per decade. More severe flooding, like the flood of 1967, which submerged downtown Cannon Beach under 2.5 ft (0.8 m) of water, probably occurred a few times per century (O'Donnell, 1996). Layer 4 met few of the criteria for a tsunami origin (Table 4). Instead, the deposit shared the mineralogical attributes of sand from the active channel of Ecola Creek (Table 2). The prevalence of sand 4 along the central axis of the valley is consistent with an overbank flood deposit, and sand 4 lacks the landward thinning trend common to tsunami deposits studied worldwide

Comparisons of the distribution of prehistoric tsunami deposits with predicted tsunami inundation lines offer an empirical test of the credibility of numerical simulations used to develop evacuation routes and for emergency response planning. The predictive power of tsunami deposits is limited because they can define only the minimum runup elevation reached by the waves and the minimum extent of inundation. However, geologic evidence of prehistoric tsunami inundation has been used to identify *tsunami simulations* that may underestimate real-world conditions; further, knowing the extents of prehistoric tsunami deposits increases confidence in model inundations that meet or exceed these extents.

***Acknowledgments***

Curt Peterson and Ken Cruikshank provided stratigraphic and survey data used in this report, some of which is compiled in an electronic data base published by Peterson and others (2008). Peterson also contributed mineralogy and grain size data for sand samples listed in Table 2. Eileen Hemphill-Haley analyzed fossil diatoms for sand layers 1, 2, and 3. Robert Schlichting provided data on fossil diatoms in sand layer 4. Al Aya and the staff at the Cannon Beach Historical Society provided assistance with historical research. Jonathan Allan measured temporary benchmarks using GPS to provide survey control. George Priest and Ian Madin provided review in the field. Portland State University students Simon Spencer, Anna Pilette, and Holly Johnson assisted with field investigations. Support for this research was provided by the Cannon Beach Rural Fire Protection District, the City of Cannon Beach, and the Clatsop County School District (Intergovernmental Agreement #41180-63006). The National Tsunami Hazard Mitigation Program, administered by the National Atmospheric and Oceanic Administration, provided additional funding (NOAA Requisition NRMAH000-6-01035) for Witter.

## REFERENCES


Atwater, B. F., 1987, Evidence for great Holocene earthquakes along the outer coast of Washington state: Science, v. 236, p. 942–944.

Atwater, B. F., and Hemphill-Haley, E., 1997, Recurrence intervals for great earthquakes of the past 3500 years at northeastern Willapa Bay, Washington: U.S. Geological Survey Professional Paper 1576, 108 p.

Atwater, B. F., Tuttle, M. P., Schweig, E. S., Rubin, C. M., Yamaguchi, D. K., and Hemphill-Haley, E., 2003, Earthquake recurrence inferred from paleoseismology, *in* A. R. Gillespie, S. C. Porter, and B. F. Atwater, eds., The Quaternary period in the United States, Developments in Quaternary science: New York, Elsevier, p. 331–350.

Benson, B. E., Grimm, K. A., and Clague, J. J., 1997, Tsunami deposits beneath tidal marshes on northwestern Vancouver Island, British Columbia: Quaternary Research, v. 48, p. 192–204.

Clague, J. J., Bobrowski, P. T., and Hutchinson, I., 2000, A review of Geological records of large tsunamis at Vancouver Island, British Columbia, and implications for hazard: Quaternary Science Reviews, v. 19, p. 849–863.

Darienzo, M. E., and Peterson, C. D., 1990, Episodic tectonic subsidence of late Holocene salt marshes, northern Oregon central Cascadia margin: Tectonics, 9, No. 1, p. 1–22.

Darienzo, M. E., and Peterson, C. D., 1995, Episodic tectonic subsidence of late Holocene salt marshes, northern Oregon central Cascadia margin: Tectonics, v. 9, p. 1–22.

Darienzo, M. E., Peterson, C. D., and Clough, C., 1994, Stratigraphic evidence for great subduction-zone earthquakes at four estuaries in northern Oregon, U.S.A.: Journal of Coastal Research, v. 10, p. 850–876.

Gallaway, P. J., Peterson, C. D., Watkins, A. M., Craig, S., and McLeod, B. L., 1992, Paleo-tsunami inundation and runup at Cannon Beach, Oregon, Final Report to Clatsop County Sheriff's Office, Oregon, Unpublished report, 47 p.

Gelfenbaum, G., and Jaffe, B., 2003, Erosion and sedimentation from the 17 July 1998 Papua New Guinea tsunami: Pure and Applied Geophysics, v. 160, p. 1,969–1,999.

Goldfinger, C., 2008, Paleoseismic slip history and geologic constraints on splay faulting and interplate coupling along the Cascadia Subduction Zone, *in* Priest, G. R., Goldfinger, C., Wang, K., Witter, R. C., Zhang, Y., and Baptista, A. M., Tsunami hazard assessment of the northern Oregon coast: A multideterministic approach tested at Cannon Beach, Clatsop County, Oregon: Oregon Department of Geology and Mineral Industries Special Paper 41.

Goldfinger, C., and Morey-Ross, A., 2004, Physical property correlations from Cascadia great earthquakes: What are they telling us about the triggering events? [Abs.]: Eos Trans. AGU Fall Meeting 945 Supl. Abstract OS21E-01, v. 85 p. 47.

Goldfinger, C., Nelson, C. H., and Johnson, J., 2003, Holocene earthquake records from the Cascadia Subduction Zone and northern San Andreas fault based on precise dating of offshore turbidites: Annual Reviews of Geophysics, v. 31, p. 555–577.

Goldfinger, C., Grijalva, K., Bürgmann, R., Morey, A., Johnson, J. E., Nelson, C. H., Gutiérrez-Pastor, J., Karabanov, E., Patton, J., and Gràcia, E., 2008, Late Holocene rupture of the northern San Andreas fault and possible stress linkage to the Cascadia Subduction Zone: Bulletin of the Seismological Society of America, in press.

Hemphill-Haley, E., 1995, Diatom evidence for earthquake-induced subsidence and tsunami 300 yr ago in southern coastal Washington: Geological Society of America Bulletin, v. 107, p. 367–378.

Hemphill-Haley, E., 1996, Diatoms as an aid in identifying late-Holocene tsunami deposits: The Holocene, v. 6, p. 439–448.

Horning, T., 2006, Appendix C. Summary of eyewitness observations from 1964 Alaska tsunami in Seaside, Oregon, *in* Tsunami Pilot Study Working Group, Seaside, Oregon tsunami pilot study – Modernization of FEMA flood hazard maps, National Oceanic and Atmospheric Administration OAR Special Report: Seattle, Washington, NOAA/OAR/PMEL, p. C1–C7.

Kelsey, H. M., Nelson, A. R., Hemphill-Haley, E., and Witter, R. C., 2005, Tsunami history of an Oregon coastal lake reveals a 4600 yr record of great earthquakes on the Cascadia subduction zone: Geological Society of America Bulletin, v. 117, no.7/8, p. 1,009–1,032.

Krammer, K., and Lange-Bertalot, H., 1991, Bacillariophyceae 3, Centrales, Fragilariaceae, Eunotiaceae, *in* Ettl, H., Gerloff, J., Heynig, H., and Mollenhauer, D., (eds), Süsswasserflora von Mitteleuropa, v. 2, no. 3: Stuttgart, Fischer.

Kraus, N.C., Militello, A., and Todoroff, G., 2002, Barrier breaching processes and barrier spit breach, Stone Lagoon, California: Shore & Beach, v. 70, no. 4, p. 21–28.

Lander, J. F., Lockridge, P. A. and Kozuch, M. J. 1993, Tsunamis affecting the West Coast of the United States, 1806-1992, KGRD No. 29: Boulder, Colorado, National Oceanic and Atmospheric Administration, National Geophysical Data Center, 242 p.

Ludwin, R.S., Dennis, R., Carver, D., McMillan, A. D., Losey, R., Clague, J., Jonientz-Trisler, C., Bowechop, J., Wray, J., and James, K., 2005, Dating the 1700 Cascadia Earthquake – Great Coastal Earthquakes in Native Stories: Seismological Research Letters, v. 76, no. 2, p. 140–148.

Moore, A, 2006, Sedimentary differences in near-source deposits of the 2004 south Asia tsunami and hurricane Katrina [abs]: Seismological Research Letters, v. 77, n. 2, p. 235.

Nelson, A. R., 1992, Discordant 14C ages from buried tidal-marsh soils in the Cascadia subduction zone, southern Oregon coast: Quaternary Research, v. 38, p. 74–90.

Nelson and 11 others, 1995, Radiocarbon evidence for extensive plate-boundary rupture about 300 years ago at the Cascadia subduction zone: Nature, v. 378, p. 371–374.

Nelson, A. R., Shennan, I., and Long, A. J., 1996, Identifying coseismic subsidence in tidal-wetland stratigraphic sequences at the Cascadia subduction zone of western North America: Journal of Geophysical Research, v. 101, no. B3, p. 6,115–6,135.

Nelson, A. R., Ota, Y., Umitsu, M., Kashima, K., and Matshushima, Y., 1998, Seismic or hydrodynamic control of rapid late-Holocene sea-level rise in southern coastal Oregon, USA?: The Holocene, v. 8, p. 287–299.

Nelson, A. R., Aspuith, A. C., and Grant, W. C., 2004, Great earthquakes and tsunamis of the past 2000 years at the Salmon River Estuary, central Oregon coast, USA: Geological Society of America, v. 94, p. 1276–1292.

Nelson, S. A., and Leclair, S. F., 2006, Katrina's unique splay deposits in a New Orleans neighborhood: GSA Today, v. 16, p. 4–10.

Niem, A., and Niem, W., 1985, Oil and gas investigation of the Astoria Basin, Clatsop and northernmost Tillamook Counties, northwest Oregon: Oregon Department of Geology and Mineral Industries, Oil and Gas Investigation 14, scale 1:100,000.

O'Donnell, T., 1996, Cannon Beach: A place by the Sea: Portland, Oregon, Oregon Historical Society Press, 164 p.

Parker, S. and the Ecola Creek Watershed Council, 2001, Ecola Creek watershed assessment: A living document: unpublished report of the Ecola Creek Watershed Council obtained on June 14, 2007 from the North Coast Watershed Association website: http://www.clatsopwatersheds.org/.

Peters, R., Jaffe, B., Gelfenbaum, G., and Peterson, C. D., 2003, Cascadia tsunami deposit database: U.S. Geological Survey Open-File Report 03-13, 24 p.

Peterson, C. D., and Darienzo, M. E., 1996, Discrimination of climatic, oceanic, and tectonic mechanisms of cyclic marsh burial: *in* Rogers, A. M., Walsh, T. J., Kockelman, W. J., and Priest, G. R., eds., Assessing earthquake hazards and reducing risk in the Pacific Northwest: USGS Professional Paper 1560, p. 115–146.

Peterson, C. D., Cruikshank, K. M., Jol, H. M., and Schlichting, R. B., 2008, Minimum runup heights of paleotsunami from evidence of sand ridge overtopping at Cannon Beach, Oregon, Central Cascadia Margin, U.S.A.: Journal of Sedimentary Research, v. 78, no. 6, 390–409.

Priest, G. R., Baptista, A. M., Flück, P., Wang, K., Kamphaus, R. A., and Peterson, C. D., 1997a, Cascadia subduction zone tsunamis: Hazard mapping at Yaquina Bay, Oregon, Final technical report to the National Earthquake Hazard Reduction Program: Oregon Department of Geology and Mineral Industries Open-File Report O-97-34, 144 p.

Priest, G. R., Myers, E., Baptista, A. M., Kamphaus, R., Peterson, C. D., and Darienzo, M. E., 1997b, Tsunami hazard map of the Yaquina Bay area, Lincoln County, Oregon: Oregon Department of Geology and Mineral Industries, Interpretive Map Series IMS-2, scale 1:12,000.

Priest, G. R., Allan, J. C., Myers, E., Baptista, A.M., and Kamphaus, R., 2002, Tsunami hazard map of the Coos Bay Area, Coos County, Oregon: Oregon Department of Geology and Mineral Industries, Interpretive Map Series IMS-21, scale 1:12,000.

Priest, G. R., Chawla, A., and Allan, J. C., 2003, Tsunami hazard map of the Alsea Bay (Waldport) area, Lincoln County, Oregon: Oregon Department of Geology and Mineral Industries, Interpretive Map Series IMS-23, scale 1:12,000.

Priest, G. R., Goldfinger, C., Wang, K., Witter, R. C., Zhang, Y., and Baptista, A. M., 2008, Tsunami hazard assessment of the northern Oregon coast: A multi-deterministic approach tested at Cannon Beach, Clatsop County, Oregon: Oregon Department of Geology and Mineral Industries Special Paper 41.

Reimer, P. J., and others, 2004, IntCal04 atmospheric radiocarbon age calibration, 26-0 ka BP: Radiocarbon, v. 46, p. 1029–1058.

Satake, K., Shimazaki, K., Tsuji, Y., and Ueda, K., 1996, Time and size of a giant earthquake in Cascadia inferred from Japanese tsunami records of January 1700: Nature, v. 379, p. 246–249.

Schatz, C. E., Curl, Jr., H., and Burt, W. V., 1964, Tsunamis on the Oregon coast: Ore Bin, v. 26, no. 12, p. 231–232.

Schlichting, R. B., and Peterson, C. D., 2006, Mapped Overland distance of paleotsunami high-velocity inundation in back-barrier wetlands of the Central Cascadia Margin, U.S.A.: Journal of Geology, v. 114, p. 577–592.

Schlicker, H. G., Deacon, R. J., Beaulieu, J. D., and Olcott, G. W., 1972, Environmental geology of the coastal region of Tillamook and Clatsop Counties, Oregon: Oregon Department of Geology and Mineral Industries Bulletin 74, 164 p., 18 maps.

Shennan, I., Long, A. J., Rutherford, M. M., Green, F. M., Innes, J. B., Lloyd, J. M., Zong, Y., and Walker, K. J., 1996, Tidal marsh stratigraphy, sea-level change and large earthquakes, I: A 5000 year record in Washington, U.S.A.: Quaternary Science Reviews, v. 15, p. 1,023–1,059.

Spaeth, M. G., and Berkman, S. C., 1967, The tsunami of March 28, 1964 as recorded at tide stations, ESSA Technical Report Coast and Geodetic Survey 33: Rockville, Maryland, U.S. Department of Commerce, 86 p.

Stuiver, M., and Reimer, P. J. ,1993, Extended 14C data base and revised CALIB 3.0 $^{14}C$ age calibration program: Radiocarbon, v. 35, p. 215–230.

Tsunami Pilot Study Working Group, 2006, Seaside, Oregon tsunami pilot study – Modernization of FEMA flood hazard maps, National Oceanic and Atmospheric Administration OAR Special Report: Seattle, WA, NOAA/OAR/PMEL, 92 p., 7 appendices.

Tuttle, M. P., Ruffman, A., Anderson, T., and Jeter, H., 2004, Distinguishing tsunami from storm deposits in eastern North America: The 1929 Grand Banks tsunami versus the 1991 Halloween storm: Seismological Research Letters, v. 75, p. 117–131.

Walsh, T. J., Caruthers, C. G., Heinitz, A. C., Myers, E. P., III, Baptista, A. M., Erdakos, G. B., and Kamphaus, R. A., 2000, Tsunami hazard map of the southern Washington coast: Modeled tsunami inundation from a Cascadia subducting zone earthquake: Washington Division of Geology and Earth Resources, Geologic Map GM-49.

Williams, H., Hutchinson, I., and Nelson, A. R., 2005, Multiple sources for late-Holocene 1169 tsunamis at Discovery Bay, Washington State, USA: The Holocene, v. 15, p. 60–73.

Witkowski, A., Lange-Bertalot, H., and Metzeltin, D., 2000, Diatom flora of marine coasts I, *in* Lange-Bertalot, H. (ed.), Iconographia Diatomologica, vol. 7: Ruggell, Liechtenstein, A.R.G. Gantner Verlag, 925 p.

Witter, R. C., Kelsey, H. M., and Hemphill-Haley, E., 2003, Great Cascadia earthquakes and tsunamis of the past 6700 years, Coquille River estuary, southern coastal Oregon: Geological Society of America Bulletin, v. 115, p. 1,289–1,306.

Zhang, Y. L., Baptista, A. M., Wang, K., Goldfinger, C., Witter, R., Priest, G., Peterson, C., and Cruikshank, K., 2007, Hydrodynamic simulations of historic tsunamis from the Cascadia subduction zone [abs.]: Portland, Oregon, Coastal Zone 2007.

# APPENDIX A: CANB43R-2 DIATOM RESULTS

The following is a summary of the diatom data for core CANB43R-2. All of the graphs are copied from Microsoft Excel file "TableA1.xls," included with this publication. The summary is organized as follows:

**Part I** – overall paleoenvironment of the core site

**Part II** – diatom concentrations (indicative of productivity, environment, or preservation), including a comparison of the concentrations of brackish-marine versus freshwater diatoms

**Part III** – occurrences of brackish-marine species, including a comparison of modern brackish-marine species and modern/Tertiary species

## Part I. General paleoecological history of the core site

To get a broad overview in possible changes in environment over time at the core site, I organized the freshwater taxa into three ecological groups (Excel file TableA1.xls). These results are not absolutely definitive and are based partly on the literature and partly on my own empirical observations at different locations from California to Alaska. However, I think there may be evidence, from changes in the freshwater assemblages, for periods of persistently wet marsh conditions (pale yellow), drier, more aerophile periods (blue), and times when the river channel strongly influenced the site (plum). The river channel environment is based on occurrences of taxa that prefer to live attached to larger plants on riverbanks.

From a literature review, I changed the designation of one species, *Diadesmis contenta*, to "riverine" instead of aerophile marsh. I have found it in high marshes around Willapa Bay, but that is probably due to lower salinity in those locations rather than ecological preference. Apparently, *Diadesmis contenta* is very commonly found in flowing water, bogs, and lakes. I think this that assigning this species to the riverine group is probably appropriate, as it is prominent in the grey-brown mud at 127.5 cm.

Again, these are not hard and fast results but possibly a broad overview of the paleoecology at the core site. I provided a list of the species I included in this rough analysis after graph 1.

## Part II. Diatom concentrations

Overall, diatom concentrations were fairly consistent between "sand" and "not-sand" samples. Concentrations are lower on average for the older samples, and although this may be an artifact of preservation, it may also have to do with having an overall environment that was not as productive for diatoms. The grey-brown mud at 127.5 cm is unique among the samples, with diatom concentrations an order of magnitude greater than the other samples.

Graph 2 compares the concentration of freshwater diatoms with total diatoms. Graph 3 shows the concentration of brackish-marine diatoms throughout the core — orders of magnitude less than concentrations of freshwater diatoms, although the overall trend is the same for both groups.

## Part III. Occurrences of brackish-marine diatoms

Although freshwater diatoms completely dominate the assemblages (as shown in Part II), total brackish-marine diatoms are fairly prominent in two samples: the lower part of sand 2 (120 cm), and the sandy peat above sand 3 (130 cm) (graphs 4 and 5). *Fragilaria schulzii* is particularly prominent in these two samples. It is a coastal species, widely distributed in Europe and North America, that grows by attaching to sand grains (Krammer and Lange-Bertalot, 1991; Witkowski and others, 2000).

Relative percentages of brackish-marine taxa are about 8 percent for sand 3 and sand 4, and 12 percent for the upper part of sand 2. I did not observe any brackish-marine species in the regular counts for sand 1. (I did some additional counts and observed a few fragments, but I do not think there is any real evidence to indicate a marine incursion.)

Most of the brackish-marine diatoms are likely modern (i.e., probably "not Tertiary"), but taxa that are either modern or Tertiary make up about 0.7–2 percent of the assemblages in five samples (graphs 5 and 6).

Note: There are no taxa that would be considered "Tertiary only." All of the "possible Tertiary" taxa in these samples could also be found in modern deposits.

Graph 6 compares "possible Tertiary" (pale yellow) and "non-Tertiary" (plum) brackish-marine diatoms relative to total brackish-marine diatoms (blue).

## REFERENCES

Krammer, K., and Lange-Bertalot, H., 1991, Bacillariophyceae 3, Centrales, Fragilariaceae, Eunotiaceae, *in* Ettl, H., Gerloff, J., Heynig, H., and Mollenhauer, D., (eds), Süsswasserflora von Mitteleuropa, v. 2, no. 3: Stuttgart, Fischer.

Witkowski, A., Lange-Bertalot, H., and Metzeltin, D., 2000, Diatom flora of marine coasts I, *in* Lange-Bertalot, H. (ed.), Iconographia Diatomologica, vol. 7: Ruggell, Liechtenstein, A.R.G. Gantner Verlag, 925 p.

**Graph 1 -- CANB43R-2: Comparison of freshwater diatom groups (relative %)**

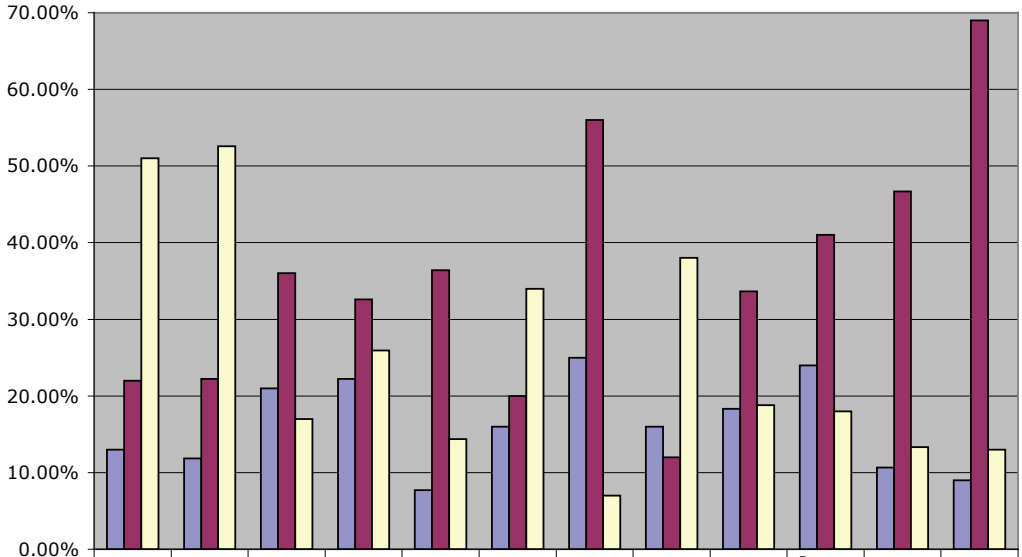


| | Brown peat | Sand 1 | Black peat | Sand 2 (upper) | Sand 2 (lower) | Brown peat | Grey-brown mud | Sandy peat | Sand 3 | Brown-grey muddy peat | Sand 4 | Grey mud |
|---|---|---|---|---|---|---|---|---|---|---|---|---|
| FW (aerophile) marsh species | 13.00% | 11.85% | 21.00% | 22.22% | 7.69% | 16.00% | 25.00% | 16.00% | 18.32% | 24.00% | 10.67% | 9.00% |
| Riverine benthic species | 22.00% | 22.22% | 36.00% | 32.59% | 36.41% | 20.00% | 56.00% | 12.00% | 33.66% | 41.00% | 46.67% | 69.00% |
| Large pinnularia + wet marsh spp. | 51.00% | 52.59% | 17.00% | 25.93% | 14.36% | 34.00% | 7.00% | 38.00% | 18.81% | 18.00% | 13.33% | 13.00% |

Table A1. Species included in analysis shown in Graph A1.

| Aerophile Marsh Species | Riverine Group | Wet Fresh Marsh Species |
|---|---|---|
| *Caloneis aerophila* | *Bacillaria paxillifer* | *Eunotia cf. valida* |
| *Caloneis bacillum* | *Cocconeis placentula* | *Eunotia incisa* |
| *Caloneis lepidula* | *Diadesmis contenta* | *Eunotia minor* |
| *Caloneis molaris* | *Diatoma hiemale v. mesodon* | *Eunotia pectinalis* |
| *Cavinula variostriata* | *Gomphonema angustum (intricatum)* | *Eunotia praerupta* |
| *Cosmioneis pusilla* | *Gomphonema augur* | *Eunotia sp.* |
| *Cymbella aspera* | *Gomphonema parvulum* | *Frustulia rhomboides* |
| *Cymbella gracilis* | *Melosira dendrophila* | *Frustulia vulgaris* |
| *Cymbella silesiaca* | *Melosira varians* | *Pinnularia aestuarii* |
| *Cymbella sinuata* | *Opephora martyi* | *Pinnularia alpina* |
| *Cymbella tumida* | *Rhoicosphenia abbreviata* | *Pinnularia gibba* |
| *Cymbella turgida* | *Surirella biseriata* | *Pinnularia major* |
| *Luticola mutica* | *Surirella robusta* | *Pinnularia microstauron* |
| *Navicula elginensis* | *Synedra ulna* | *Pinnularia obscura* |
| *Navicular peregrinopsis* | | *Pinnularia viridis* |
| *Navicula rhyncocephala* | | *Stauroneis anceps* |
| *Navicula slesvicensis* | | *Stauroneis kriegeri* |
| *Nitzschia terrestris* | | *Stauroneis phoenicenteron* |
| Pinnularia lagerstedtii | | |
| Sellaphora pupula | | |

**Graph 2 -- CANB43R-2: Total vs. freshwater diatom concentration (valves/cc of sediment)**

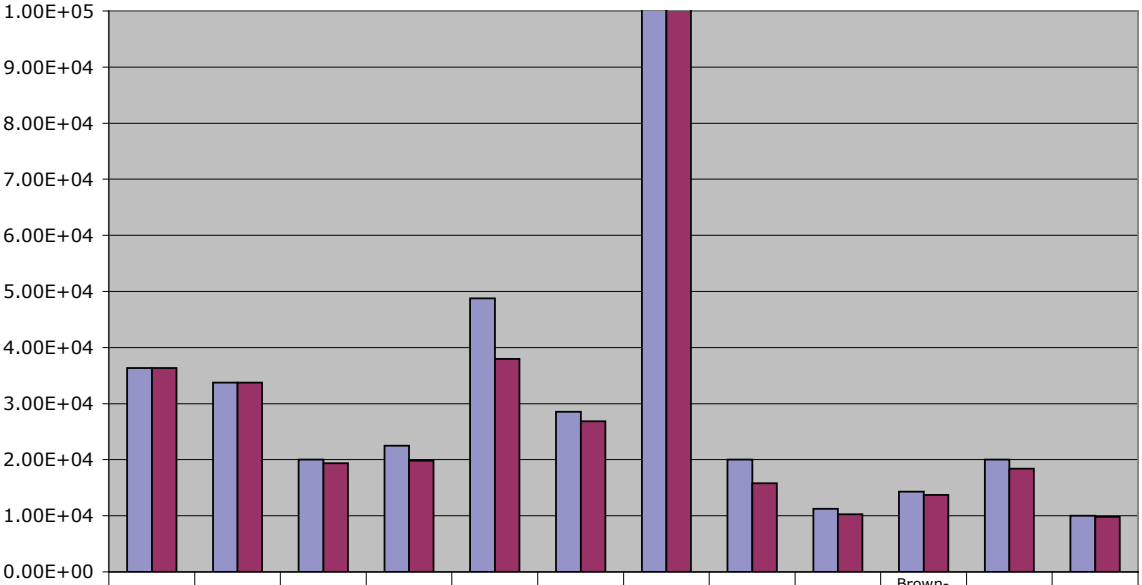


| | Brown peat | Sand 1 | Black peat | Sand 2 (upper) | Sand 2 (lower) | Brown peat | Grey-brown mud | Sandy peat | Sand 3 | Brown-grey muddy peat | Sand 4 | Grey mud |
|---|---|---|---|---|---|---|---|---|---|---|---|---|
| Total valves/cc | 3.64E+04 | 3.38E+04 | 2.00E+04 | 2.25E+04 | 4.88E+04 | 2.86E+04 | 2.67E+05 | 2.00E+04 | 1.12E+04 | 1.43E+04 | 2.00E+04 | 1.00E+04 |
| Total FW diatoms/cc | 3.64E+04 | 3.38E+04 | 1.94E+04 | 1.98E+04 | 3.80E+04 | 2.69E+04 | 2.51E+05 | 1.58E+04 | 1.03E+04 | 1.37E+04 | 1.84E+04 | 9.80E+03 |

**Graph 3 -- CANB43R-2: Concentration of brackish-marine diatoms (valves/cc of sediment)**

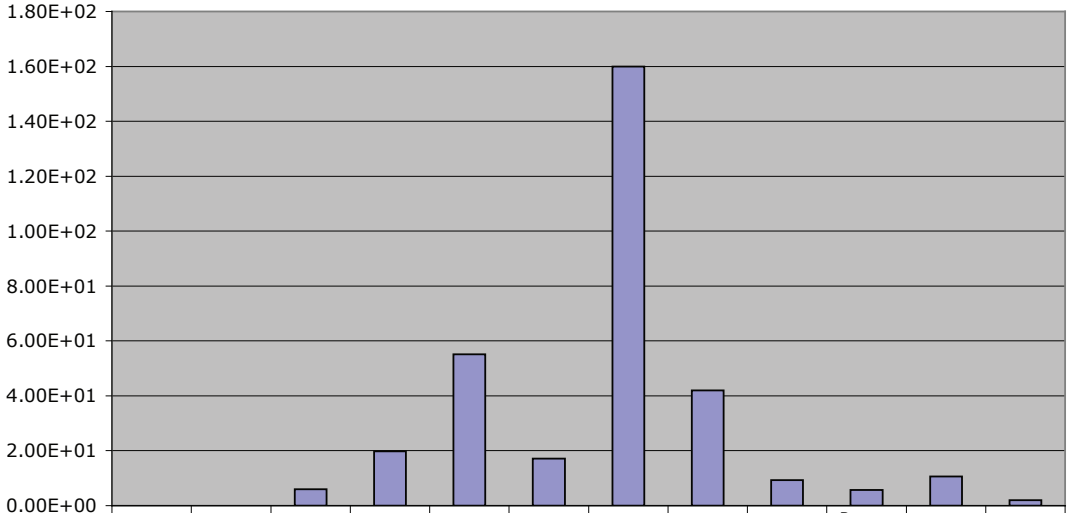


| | Brown peat | Sand 1 | Black peat | Sand 2 (upper) | Sand 2 (lower) | Brown peat | Grey-brown mud | Sandy peat | Sand 3 | Brown-grey muddy peat | Sand 4 | Grey mud |
|---|---|---|---|---|---|---|---|---|---|---|---|---|
| Total brack-marine diatoms/cc | 0.00E+00 | 0.00E+00 | 6.00E+00 | 1.98E+01 | 5.51E+01 | 1.71E+01 | 1.60E+02 | 4.20E+01 | 9.35E+00 | 5.71E+00 | 1.07E+01 | 2.00E+00 |

**Graph 4 -- CANB43R-2: Freshwater vs. Brack-Marine diatoms (relative %)**

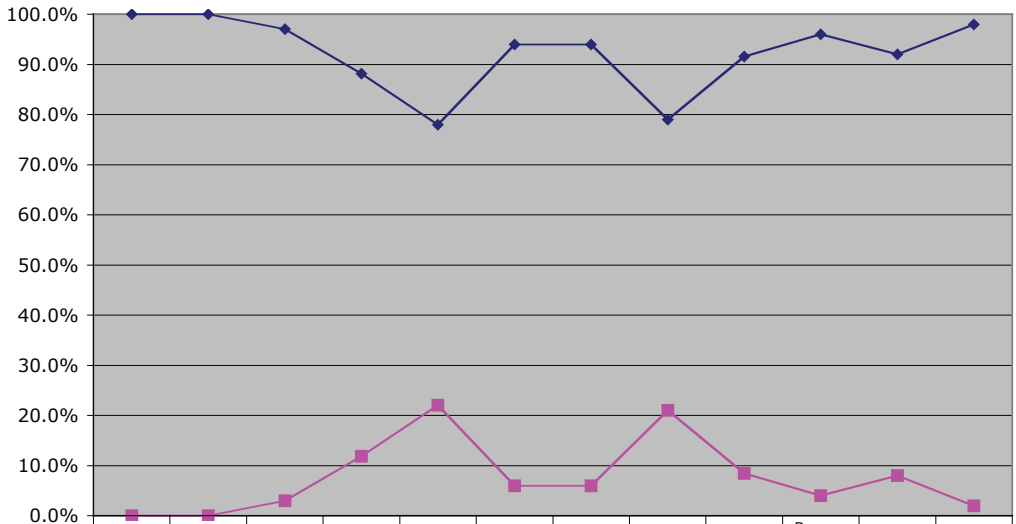


| | Brown peat | Sand 1 | Black peat | Sand 2 (upper) | Sand 2 (lower) | Brown peat | Grey-brown mud | Sandy peat | Sand 3 | Brown-grey muddy peat | Sand 4 | Grey mud |
|---|---|---|---|---|---|---|---|---|---|---|---|---|
| Freshwater diatoms | 100.0% | 100.0% | 97.0% | 88.1% | 77.9% | 94.0% | 94.0% | 79.0% | 91.6% | 96.0% | 92.0% | 98.0% |
| Total brackish-marine diatoms | 0.0% | 0.0% | 3.0% | 11.9% | 22.1% | 6.0% | 6.0% | 21.0% | 8.4% | 4.0% | 8.0% | 2.0% |

**Graph 5 -- CANB43R-2: Comparison of freshwater and brackish-marine diatoms, showing modern ("non-Tertiary") and "possible Tertiary" taxa (relative %)**

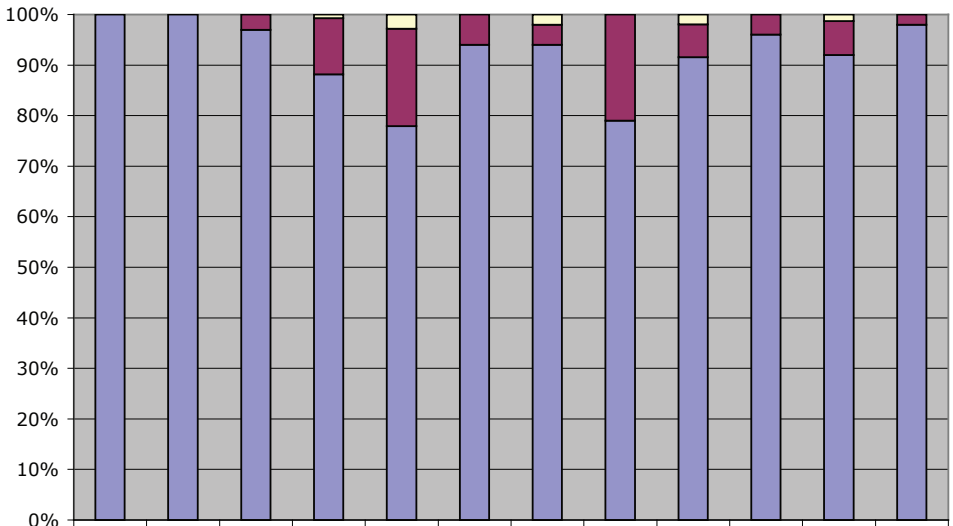


| | Brown peat | Sand 1 | Black peat | Sand 2 (upper) | Sand 2 (lower) | Brown peat | Grey-brown mud | Sandy peat | Sand 3 | Brown-grey muddy peat | Sand 4 | Grey mud |
|---|---|---|---|---|---|---|---|---|---|---|---|---|
| Possible Tertiary brackish-marine species | 0.0% | 0.0% | 0.0% | 0.7% | 2.8% | 0.0% | 2.0% | 0.0% | 2.0% | 0.0% | 1.3% | 0.0% |
| Non-Tertiary brackish-marine species | 0.0% | 0.0% | 3.0% | 11.1% | 19.2% | 6.0% | 4.0% | 21.0% | 6.4% | 4.0% | 6.7% | 2.0% |
| Freshwater diatoms | 100.0% | 100.0% | 97.0% | 88.1% | 77.9% | 94.0% | 94.0% | 79.0% | 91.6% | 96.0% | 92.0% | 98.0% |

**Graph 6 -- CANB43R-2: Comparison of total brackish-marine diatoms with non-Tertiary species and possible Tertiary species**

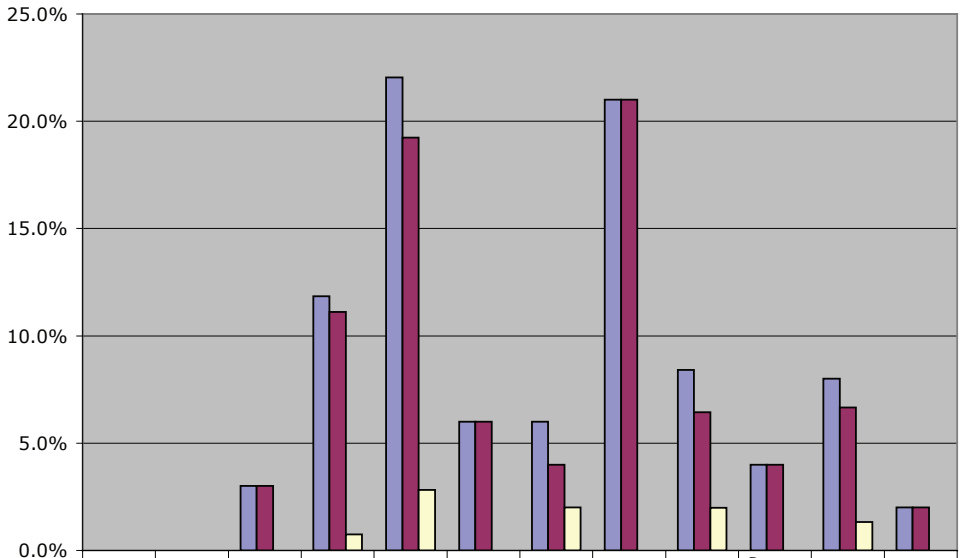


| | Brown peat | Sand 1 | Black peat | Sand 2 (upper) | Sand 2 (lower) | Brown peat | Grey-brown mud | Sandy peat | Sand 3 | Brown-grey muddy peat | Sand 4 | Grey mud |
|---|---|---|---|---|---|---|---|---|---|---|---|---|
| Total brackish-marine diatoms | 0.0% | 0.0% | 3.0% | 11.9% | 22.1% | 6.0% | 6.0% | 21.0% | 8.4% | 4.0% | 8.0% | 2.0% |
| Non-Tertiary brackish-marine species | 0.0% | 0.0% | 3.0% | 11.1% | 19.2% | 6.0% | 4.0% | 21.0% | 6.4% | 4.0% | 6.7% | 2.0% |
| Possible Tertiary brackish-marine species | 0.0% | 0.0% | 0.0% | 0.7% | 2.8% | 0.0% | 2.0% | 0.0% | 2.0% | 0.0% | 1.3% | 0.0% |